J. Fluid Mech. (1991), *vol.* 227, *pp.* 357–391
Printed in Great Britain

Instability of stationary unbounded stratified fluid

By G. K. BATCHELOR AND J. M. NITSCHE†
Department of Applied Mathematics and Theoretical Physics, University of Cambridge, Silver Street, Cambridge CB3 9EW, UK

(Received 20 July 1990)

Suppose that the density of stationary unbounded viscous fluid is a sinusoidal function of the vertical position coordinate z. Is this body of fluid gravitationally unstable to small disturbances, and, if so, under what conditions, and to what type of disturbance? These questions are considered herein, and the answers are that the fluid is indeed unstable, for any non-zero value of the amplitude of the sine wave, to disturbances with large horizontal wavelength. These disturbances have approximately vertical velocity everywhere and tilt the alternate layers of heavier and of lighter fluid, causing the fluid in the former to slide down and that in the latter to slide up, leading to a sinusoidal variation of the vertically averaged density and thereby to reinforcement of the vertical motion. The identification of this novel and efficient global instability mechanism prompts a consideration of the stability of other cases of unbounded fluid stratified in layers. Two other types of undisturbed density distribution, the first an isolated central layer of heavier or lighter fluid, with density varying say as a Gaussian function, and the second an isolated layer of fluid in which the density varies as the derivative of a Gaussian function, are found to be unstable, at all values of the magnitude of the density variation, to disturbances having the same global character. For the first of these two types of density distribution, the behaviour of a disturbance with long horizontal wavelength depends only on the net excess mass of unit area of the central layer, and for the second it depends only on the first moment of the density in the central layer. For the second type there arises another global instability mechanism in which light fluid is stripped away from one side of the layer and heavy fluid from the other without any tilting. In all cases the properties of a neutral disturbance are determined numerically, and the growth rate is found as a function of the Rayleigh number, the Prandtl number, and the horizontal wavenumber of the disturbance. An energy argument gives results easily for the inviscid non-diffusive limit, when all disturbances grow, and reveals the tilting-sliding mechanism of the instability of a disturbance with large horizontal wavelength in its simplest form.

1. Introduction

Most of the known results concerning the gravitational stability of stationary stratified fluid refer to fluid confined between two horizontal plane boundaries. In this paper we consider the stability of stationary fluid which by contrast extends to infinity in the vertical direction with a specified continuous distribution of density. For simplicity here we shall suppose the fluid to be completely unbounded, but the distinguishing feature of the cases considered is that there are no horizontal boundaries present. The absence of horizontal boundaries allows vertical disturbance

† Now at Department of Chemical Engineering, State University of New York at Buffalo, Buffalo, NY 14260, USA.

velocities of the same sign over large ranges of values of the vertical coordinate z, and we shall see that this is a common property of the disturbances to which the fluid is most unstable. There are some novel features of the instability of stratified fluid in the absence of horizontal boundaries, and we have thought it worthwhile to take a general point of view and to study the stability properties of classes of vertical density distribution. Throughout the paper we consider only small disturbances governed by linear equations.

The particular question that drew our attention to problems of stability of stratified flow without horizontal boundaries arises in the theory of sedimentation waves in dispersions of small particles (Batchelor 1991). It is known from the work of Kynch (1952) that, when the concentration of particles varies so slowly with respect to z that the local mean fall speed of particles is approximately the same function of local concentration as in a statistically homogeneous dispersion, a sinusoidal variation of concentration with small amplitude propagates vertically (as a kinematic wave) without change of form. Jackson (1963) subsequently showed that inclusion of the effect of particle inertia in the equations governing such a wave leads to growth of the wave amplitude. There are other effects, not considered by Jackson in this early work, which are stabilizing, but later studies (Batchelor 1988) have established that the destabilizing effect of particle inertia is dominant under certain conditions which are realizable physically. Thus the amplitude of a sinusoidal sedimentation wave with horizontal wave front may grow exponentially with time in a fluidized bed. There arises then the question: since the mean density distribution in a sedimentation wave is statically unstable in every alternate half-wavelength, is there a secondary overturning instability which sets in when the wave amplitude exceeds a certain value? Inasmuch as a dispersion of small particles in fluid with non-uniform concentration behaves dynamically like a continuum with non-uniform density when the speed of fall of a particle relative to the fluid locally is sufficiently small, we may expect to be able to give a partial answer to this question from results for the instability of a continuum with a sinusoidal density distribution. To go further and to allow for the effect of the relative motion of the fluid and the particles would take us into considerations of two-phase flow theory which do not have a natural place in this paper, so we shall not pursue this potential application of the stability theory here. The purpose in mentioning it is to indicate the original motivation for our work.

It will be supposed herein that the fluid is viscous and that the conserved quantity affecting the fluid density (e.g. heat, mass of solute, number of suspended particles) diffuses through the fluid. We shall wish for convenience to be able to make the conventional assumption of hydrodynamic stability theory that the undisturbed state is steady, and we are aware that the only vertical distribution of density with which this is exactly compatible in the absence of sources of buoyancy is one with uniform density gradient. Even so, we shall suppose that some other density distributions may exist in the undisturbed state. In some cases one can give an *a priori* justification for supposing that the specified density distribution in the undisturbed fluid is approximately steady. For example, Matthews (1988) invoked the effect of solar heating of the surface layers of a lake to justify the steadiness of his assumed cubic density profile; and the sedimentation waves mentioned above are known to have steady amplitude under certain conditions. In other cases the justification may be *a posteriori* inasmuch as one finds that the disturbance has growth timescales small compared with the time for significant change of the density profile by diffusion or has lengthscales large compared with the distance over which

appreciable diffusion occurs. There are various possibilities, and they are best considered in a specific context after the results for the assumed steady density distributions are available.

After setting out the usual equations governing a small disturbance of a stratified fluid (§2), we determine the rate of growth of a disturbance of arbitrary form when the undisturbed vertical density gradient is uniform and positive (§3). We then begin the discussion of undisturbed density gradients which are non-uniform, taking first the case studied by Gribov & Gurevich (1957) and Matthews (1988) in which the density gradient is negative everywhere except within a layer of finite thickness (§4). The absence of horizontal boundaries is not of major significance here, because the static stability of the fluid outside the layer prevents up or down currents of large vertical extent in any event. It is crucial however in the case in which the fluid density is a sinusoidal function of z in the undisturbed state (§5). Up or down currents of large vertical extent also play an important role when the density is uniform outside a central layer with the same values on the two sides and there are various types of density distribution within the layer (§6). The main contribution of this paper is the discovery that in all these new cases there are global types of disturbance with large horizontal wavelength which are not associated closely with local regions of static instability and which grow exponentially however small the magnitude of the variation of density in the undisturbed state. An energy argument which is applicable to fluid with zero viscosity and density diffusivity reveals one of the global instability mechanisms clearly (§7). Both at low and at high Reynolds numbers of the disturbance motion the precise form of the density distribution within the layers has only a secondary influence on the stability properties.

2. Equations governing a small disturbance to stationary stratified fluid

The fluid density and pressure in the undisturbed stationary state will be written as

$$\rho_0+\rho_1(z), \quad p_0-g\int(\rho_0+\rho_1)\,\mathrm{d}z,$$

where ρ_0 and p_0 are representative values. The vertical coordinate z is positive upwards. In the disturbed state the fluid velocity is $\boldsymbol{u}$, with components u, v, w, and the density and pressure are

$$\rho=\rho_0+\rho_1+\rho', \quad p=p_0-g\int(\rho_0+\rho_1)\,\mathrm{d}z+p'.$$

The equation of motion for the fluid, assumed to have uniform viscosity μ, is then

$$\rho\left(\frac{\partial \boldsymbol{u}}{\partial t}+\boldsymbol{u}\cdot\boldsymbol{\nabla}\boldsymbol{u}\right)=\rho'\boldsymbol{g}-\boldsymbol{\nabla}p'+\mu\nabla^2\boldsymbol{u}. \tag{2.1}$$

If now we assume $|\rho_1+\rho'|\ll\rho_0$ and make the Boussinesq approximation that density variations are significant only through their influence on the gravitational force, the density ρ multiplying the fluid acceleration in (2.1) may be replaced by ρ_0 and the mass-conservation relation reduces to

$$\boldsymbol{\nabla}\cdot\boldsymbol{u}=0. \tag{2.2}$$

The linearized form of (2.1) is then

$$\rho_0\frac{\partial \boldsymbol{u}}{\partial t}=\rho'\boldsymbol{g}-\boldsymbol{\nabla}p'+\mu\nabla^2\boldsymbol{u}. \tag{2.3}$$

The variation of fluid density is normally a consequence of non-uniformity of the intensity of some conserved physical quantity such as heat or mass of solute or number of small suspended particles. This conserved quantity is convected with the fluid and may also be diffused relative to the fluid. If we assume that the diffusivity D is uniform, the conservation equation for the intensity C (standing for temperature or concentration) in incompressible fluid in the absence of external sources is

$$\frac{\partial C}{\partial t}+\boldsymbol{u}\cdot\boldsymbol{\nabla}C = D\nabla^2 C. \tag{2.4}$$

The relation between ρ and C is linear for small variations in ρ and may be written as

$$\rho-\rho_0 = \beta(C-C_0), \tag{2.5}$$

where β is a constant dependent on the physical meaning of C. Equation (2.4) then becomes

$$\frac{\partial(\rho_1+\rho')}{\partial t}+\boldsymbol{u}\cdot\boldsymbol{\nabla}(\rho_1+\rho') = D\nabla^2(\rho_1+\rho'). \tag{2.6}$$

This is the point at which we make the assumptions (i) that equation (2.6) is satisfied in the undisturbed state when the fluid is stationary, whence

$$\frac{\partial\rho_1}{\partial t} = D\frac{\partial^2\rho_1}{\partial z^2}, \tag{2.7}$$

and (ii) that the undisturbed state is steady, whence $\partial\rho_1/\partial t = 0$. These two assumptions are exactly compatible only if $\partial\rho_1/\partial z$ is uniform. As explained in the introduction we shall ignore the inconsistency involved in the adoption of nonlinear density profiles and leave for later *ad hoc* consideration the question whether in a particular case there is a distributed source of buoyancy in the fluid, represented by an additional term on the right-hand side of (2.7) which is equal and opposite to $D\partial^2\rho_1/\partial z^2$, or whether both terms in (2.7) are of small magnitude in some appropriate sense, or whether the consequences of these magnitudes not being small are immaterial for certain purposes. The linearized form of (2.6), after use of (2.7), is then

$$\frac{\partial\rho'}{\partial t}+w\frac{\mathrm{d}\rho_1}{\mathrm{d}z} = D\nabla^2\rho'. \tag{2.8}$$

Equations (2.2), (2.3) and (2.8) govern the behaviour of a small disturbance to an undisturbed state in which the fluid is stationary and the density ρ_1 depends on z alone. The dependent variables u, v, ρ', p' may be eliminated from these equations, giving

$$\left(\frac{\partial}{\partial t}-D\nabla^2\right)\left(\frac{\partial}{\partial t}-\nu\nabla^2\right)\nabla^2 w = \frac{g}{\rho_0}\frac{\mathrm{d}\rho_1}{\mathrm{d}z}\nabla_{\mathrm{h}}^2 w \tag{2.9}$$

as the equation for the vertical velocity component w, where $\nu = \mu/\rho_0$ and ∇_{h}^2 denotes the Laplacian operator in the horizontal plane.

We shall assume the existence of normal modes of disturbance, and suppose all disturbance quantities associated with one mode to be proportional to $\exp(\gamma t)$. In the absence of bulk rotation and externally imposed magnetic fields and other effects causing oscillatory behaviour of an overturning disturbance, it seems clear on

physical grounds that γ must be real for a neutral or growing disturbance; and a formal proof for the case of fluid with uniform density gradient in a vertical tube has been given by Yih (1959). We shall take it for granted that a neutral disturbance is characterized by $\gamma = 0$, and so is steady, for all the different forms of the function $\rho_1(z)$ considered here.

In the absence of vertical boundaries Fourier components of the disturbance with respect to a horizontal coordinate x are independent. Hence for a normal mode we may write

$$w = W(z)\,\mathrm{e}^{\gamma t}\cos\alpha x, \quad \rho', p' \propto \mathrm{e}^{\gamma t}\cos\alpha x, \quad u \propto \mathrm{e}^{\gamma t}\sin\alpha x, \tag{2.10}$$

so that (2.9) becomes

$$\left(\frac{\gamma}{D}+\alpha^2-\frac{\mathrm{d}^2}{\mathrm{d}z^2}\right)\left(\frac{\gamma}{\nu}+\alpha^2-\frac{\mathrm{d}^2}{\mathrm{d}z^2}\right)\left(\alpha^2-\frac{\mathrm{d}^2}{\mathrm{d}z^2}\right)W = \frac{g\alpha^2}{D\nu\rho_0}\frac{\mathrm{d}\rho_1}{\mathrm{d}z}W. \tag{2.11}$$

We resist the temptation to make the variables dimensionless at this stage, because the choice of the required representative length depends on the particular undisturbed density distribution. Definition of the Rayleigh number as a governing parameter likewise must wait.

Solutions of (2.11) will now be considered for different functional forms of $\mathrm{d}\rho_1/\mathrm{d}z$.

3. A uniform undisturbed density gradient

This is the classical case on which previous work on instability of stationary stratified fluid has concentrated. However it seems not to have been noticed in the literature that there is a simple explicit solution for the stability exponent γ in the case in which there are no boundaries and the fluid extends to infinity in all directions.

All coefficients in the disturbance equation (2.11) are constant here, so Fourier components of W with respect to z are independent. We thus lose no generality by writing

$$W, \rho' \propto \cos\kappa z, \quad u, p' \propto \sin\kappa z \tag{3.1}$$

and substituting in (2.11) to obtain

$$\left(\frac{\gamma}{D}+\alpha^2+\kappa^2\right)\left(\frac{\gamma}{\nu}+\alpha^2+\kappa^2\right)(\alpha^2+\kappa^2) = \frac{g\alpha^2}{D\nu\rho_0}\frac{\mathrm{d}\rho_1}{\mathrm{d}z}. \tag{3.2}$$

One root of this quadratic equation for γ is

$$\gamma = \tfrac{1}{2}(\kappa^2+\alpha^2)[\{D-\nu)^2+4D\nu S\}^{\frac{1}{2}}-(D+\nu)], \tag{3.3}$$

showing that the disturbance grows exponentially (γ real and positive) if

$$S = \frac{\alpha^2}{(\kappa^2+\alpha^2)^3}\frac{g}{D\nu\rho_0}\frac{\mathrm{d}\rho_1}{\mathrm{d}z} > 1. \tag{3.4}$$

We see that for given α the smallest positive value of $\mathrm{d}\rho_1/\mathrm{d}z$ for which a disturbance grows occurs at $\kappa = 0$, corresponding to a disturbance mode with straight vertical streamlines for which the nonlinear terms in the full governing equations are identically zero. This is the first appearance of the common result that, in the absence of horizontal boundaries, up and down currents extending over large

vertical distances provide a very efficient way of releasing the potential energy of the undisturbed state. The value of the smallest undisturbed density gradient for a neutral disturbance with horizontal wavenumber α is thus

$$\frac{1}{\rho_0}\left(\frac{\mathrm{d}\rho_1}{\mathrm{d}z}\right)_{\gamma=0,\,\kappa=0} = \frac{\alpha^4 D\nu}{g}. \tag{3.5}$$

This simple case provides a standard with which critical gradients for other undisturbed states may be compared.

4. Fluid with a statically stable density distribution except in a central layer

There have been several studies of the instability of stationary fluid with a non-uniform density gradient in the context of what in geophysics is referred to as 'penetrative convection'. This arises in systems where a fluid layer with positive vertical density gradient adjoins at least one semi-infinite region of fluid with negative density gradient. Roll motions driven by the unstable central layer are generally found to extend well into the stable regions, hence the name. Two of these studies which have some relevance to the present work, by Matthews (1988) and by Gribov & Gurevich (1957), will be described briefly here.

Matthews (1988) considered the case of unbounded fluid in which the undisturbed density, regarded as a steady distribution maintained by a solar volumetric heat source, takes the form of a cubic polynomial in z:

$$\frac{\rho_1(z)}{\rho_0} = \frac{Az}{d}\left[1-\left(\frac{z}{d}\right)^2\right]. \tag{4.1}$$

The appropriate Rayleigh number here is $R = gAd^3/D\nu$. The density gradient $\mathrm{d}\rho_1/\mathrm{d}z$ is positive for $|z| < d/\sqrt{3}$, and the density $\rho_0+\rho_1$ takes the base value ρ_0 at $z = 0$ and $z = \pm d$ (figure 1*a*). Matthews solved the eigenvalue problem (2.11) with $\gamma = 0$ by taking the Fourier transform with respect to z, which leads to a second-order differential equation with variable coefficients for the transform $\hat{W}(\omega)$ in consequence of the quadratic dependence of the density gradient on z. The value of R is determined by Runge-Kutta shooting from $\omega = 0$ subject to the requirement that $\hat{W} = 0$ at some large value of ω, as a numerical implementation of the condition that $\hat{W}(\omega)\to 0$ as $\omega\to\infty$. The Rayleigh number for a neutral disturbance depends on the wavenumber α and is found to have a minimum value of 88.0 at $\alpha d = 1.26$ (in the case of the first mode for which W is an even function of z – the minimum value of R for the first odd mode is several times as large). Numerical inversion of $\hat{W}$ leads to streamlines exhibiting a surprisingly large central roll in the interval $|z| < 1.69d$, extending well beyond the confines of the statically unstable layer, and symmetrical sequences of rolls of rapidly diminishing flow strength above and below. On physical grounds some penetration is expected, since a fluid element with the local maximum density at $z = d/\sqrt{3}$ experiences a downward gravitational force until it reaches fluid of the same density at $z = -2d/\sqrt{3}$.

With regard to both the primary roll structure and the feature of a minimum value of R at a non-zero horizontal wavenumber, the cubic density stratification is identical in its qualitative features with other systems (e.g. the Bénard flow cell) where horizontal planar boundaries or other constraints prevent upflow and downflow currents from extending to infinity. The negative density gradients in the semi-

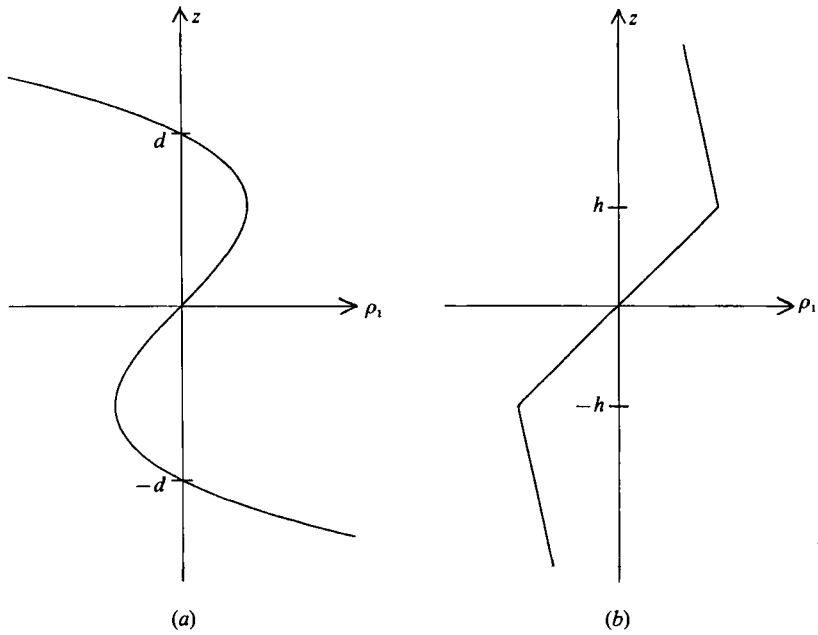

FIGURE 1. Fluid with a statically stable density distribution except in a central layer. (*a*) The cubic dependence on z considered by Matthews (1988); (*b*) the piecewise-linear dependence on z considered by Gribov & Gurevich (1957).

infinite regions outside the central layers here effectively confine disturbance flow to a region whose vertical extent is of the same order of magnitude as the thickness of the statically unstable layer.

Quantitative information related to this observation is provided by Matthews' additional consideration of the influence of constant-density free or rigid boundaries at $z = \pm \mathscr{L}$. For free boundaries he expands W in the cosine series

$$W = \sum_{k=1}^{\infty} W_k \cos\left[\pi(k-\tfrac{1}{2})\, z/\mathscr{L}\right], \tag{4.2}$$

which satisfies the pertinent boundary conditions. The coefficients W_k are governed by an infinite homogeneous system of linear equations, which yields a matrix eigenvalue problem. Matthews obtained numerical approximations for R by truncating the linear system at various orders, the largest being 4×4, and finding the smallest value of R for which the determinant vanishes. Among other conclusions, the calculations demonstrate that the minimum Rayleigh number for a neutral disturbance for $\mathscr{L}/d = 3$ is already close to the corresponding value for the original unbounded system, the intervening statically stable layers having effectively damped out the flow before it can reach the boundaries. Calculations for rigid boundaries yield the same qualitative conclusion.

Previous analyses of penetrative instabilities have often addressed continuous, piecewise-linear density distributions which necessarily possess corners, requiring delta-function sources and sinks of buoyancy in the fluid (figure 1*b*). There exists an early analysis of this type by Gribov & Gurevich (1957) which bears some relation to the developments described in §§5, 6. Among other calculations, these authors considered the limiting case in which the non-dimensional density gradients in the

semi-infinite statically stable regions above and below the central layer (C_1 and C_2 in their notation), now considered to be parameters independent of the gradient in the central statically unstable layer, are equal and tend to zero. As expected, for fixed C_2 the Rayleigh number (based on properties of the central layer of thickness h) for a neutral disturbance exhibits a minimum R_m at a certain value of the horizontal wavenumber α_m. The results have the intriguing feature that, in the limit as $C_2 \to 0$, (i) both R_m and α_m tend to zero, and (ii) the depth of penetration of the corresponding convective rolls (their h^*) is inversely proportional to α_m and therefore increases without bound. The latter statement indicates that the vertical extent of the disturbance flow is no longer limited, in order of magnitude, to the thickness of the central layer. The precise scaling dependences, extracted from their equations (45) and (46), are as follows:

$$R_m \sim 34(h\alpha_m)^3 \quad \text{and} \quad h^* \sim 2.4/\alpha_m, \quad \text{where} \quad h\alpha_m \sim 0.60C_2^{\frac{1}{4}}. \tag{4.3}$$

Gribov & Gurevich give little indication of the form of the disturbance flow, and their analysis is so complex mathematically that the physical significance of these asymptotic relations is concealed.

Neutral disturbances for which R and α are both small constitute a central feature of our new work. In the next two sections we present an analysis of 'global' disturbances that uncovers the driving physical mechanism and illuminates its key asymptotic features.

5. A sinusoidal undisturbed density distribution

This is the case that initially motivated our study of instability of stratified fluid in the absence of horizontal boundaries. As explained in the introduction, a sinusoidal vertical distribution of particle concentration may arise spontaneously in a fluidized bed under certain conditions, and it is of interest to know whether and when this sinusoidal distribution with growing amplitude becomes unstable to overturning disturbances. Provided the relative velocity of particles and the surrounding fluid is small, it seems likely that this overturning instability may be investigated on the assumption that the mixture of particles and fluid behaves as a new continuous fluid with the same mean density. Whether that assumption is valid, and the consequences for the stability properties if it is not, are matters for future investigation from two-phase flow theory. Here we consider only the overturning instability of a continuous fluid and leave aside the possible application to fluidized beds.

The undisturbed density will be written as

$$\rho_0 + \rho_1 = \rho_0(1 + A\sin\kappa z)$$

in which the constant A is positive. A suitable definition of the Rayleigh number is then

$$R = \frac{gA}{D\nu\kappa^3}. \tag{5.1}$$

As before we suppose that the fluid is unbounded in all directions. The general form of the disturbance is given by (2.10), and the governing differential equation (2.11) becomes

$$\left(\frac{\gamma}{D} + \alpha^2 - \frac{\mathrm{d}^2}{\mathrm{d}z^2}\right)\left(\frac{\gamma}{\nu} + \alpha^2 - \frac{\mathrm{d}^2}{\mathrm{d}z^2}\right)\left(\alpha^2 - \frac{\mathrm{d}^2}{\mathrm{d}z^2}\right) W = \alpha^2\kappa^4 R\cos\kappa z\, W. \tag{5.2}$$

The standard eigenvalue methods for equations with constant coefficients are not applicable, but we can exploit the expectation that there are solutions for which W is a periodic function of z with period $2\pi/\kappa$ and use solution techniques like those applicable to Mathieu's equation. We write

$$W(z) = \sum_{n=1}^{\infty} F_n \sin n\kappa z + \sum_{n=0}^{\infty} G_n \cos n\kappa z, \tag{5.3}$$

then substitute in (5.2), convert all terms in (5.2) to Fourier series, and equate coefficients. The odd and even functions of z in (5.3) are not coupled, and so we may consider them separately, taking the odd sine series first. Note that, as the origin of z has been chosen, ρ_1 is an odd function of z.

5.1. *Disturbance modes with W odd in z*

The odd part of equation (5.2) is

$$\sum_{n=1}^{\infty} L_n F_n \sin n\kappa z = \tfrac{1}{2}\alpha^2\kappa^4 R \sum_{n=1}^{\infty} F_n\{\sin(n-1)\kappa z + \sin(n+1)\kappa z\},$$

where

$$L_n = \left(\frac{\gamma}{D} + \alpha^2 + n^2\kappa^2\right)\left(\frac{\gamma}{\nu} + \alpha^2 + n^2\kappa^2\right)(\alpha^2 + n^2\kappa^2), \tag{5.4}$$

and equating coefficients of $\sin n\kappa z$ gives

$$L_n F_n = \tfrac{1}{2}\alpha^2\kappa^4 R(F_{n-1} + F_{n+1}) \quad (n = 1, 2, \ldots), \tag{5.5}$$

in which $F_0 = 0$. We note that L_n increases rapidly with n, which suggests that F_n decreases rapidly and that an approximate solution of this three-term recurrence relation may be obtained by truncating the Fourier series for $W(z)$.

In the extreme case in which we put $F_n = 0$ for $n > 2$, (5.5) reduces to the two equations

$$L_1 F_1 = \tfrac{1}{2}\alpha^2\kappa^4 R F_2, \quad L_2 F_2 = \tfrac{1}{2}\alpha^2\kappa^4 R F_1, \tag{5.6}$$

and the existence of a non-zero solution for F_1 and F_2 requires

$$\tfrac{1}{2}\alpha^2\kappa^4 R = (L_1 L_2)^{\frac{1}{2}}. \tag{5.7}$$

If instead we put $F_n = 0$ for $n > 3$, we find that the right-hand side of (5.7) is multiplied by the factor $L_3^{\frac{1}{2}}/(L_1 + L_3)^{\frac{1}{2}}$, which is not very different from unity. The next approximation, obtained by putting $F_n = 0$ for $n > 4$, gives

$$(\tfrac{1}{2}\alpha^2\kappa^2 R)^4 - (L_1 L_2 + L_1 L_4 + L_3 L_4)(\tfrac{1}{2}\alpha^2\kappa^4 R)^2 + L_1 L_2 L_3 L_4 = 0, \tag{5.8}$$

of which there are now two roots for R. Since $L_1 L_4$ is small compared with $L_3 L_4$, the two roots are approximately

$$\tfrac{1}{2}\alpha^2\kappa^4 R = (L_1 L_2)^{\frac{1}{2}}, \quad \tfrac{1}{2}\alpha^2\kappa^4 R = (L_3 L_4)^{\frac{1}{2}}, \tag{5.9}$$

which repeats the earlier estimate of the smaller root. Truncation at larger values of n similarly confirms estimates of the smaller roots and adds new larger roots.

Setting $F_n = 0$ for n larger than some small integer, as above, has the advantage of giving simple explicit approximate formulae. Our numerical results, however, are all obtained from truncations after $n = 10$ and machine calculations by standard methods, and can be considered to be 'exact'. As it turns out, the approximate formulae are very accurate quantitatively.

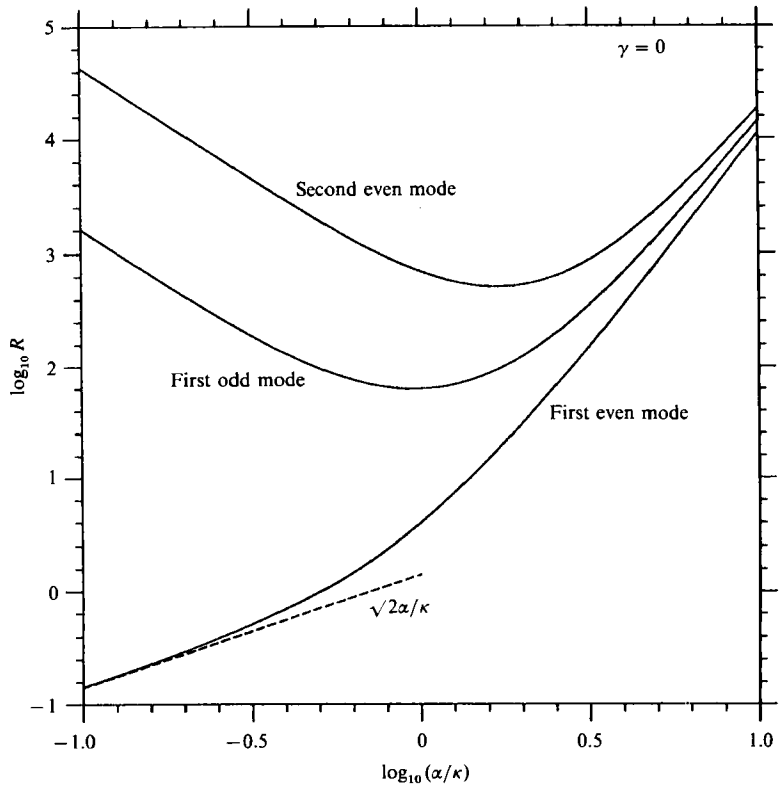

FIGURE 2. Rayleigh number as a function of the horizontal wavenumber α for either odd or even modes of a neutral disturbance to stationary fluid with density varying sinusoidally with respect to z.

Each solution of the characteristic equation represents a relation between the dimensionless quantities

$$R, \quad \frac{\gamma}{(D\nu)^{\frac{1}{2}}\kappa^2}, \quad \frac{\nu}{D}, \quad \frac{\alpha}{\kappa}.$$

For a neutral disturbance ($\gamma = 0$), the dependence on ν/D disappears and (5.9) reduces to

$$R = \frac{(\kappa^2+\alpha^2)^{\frac{3}{2}}(4\kappa^2+\alpha^2)^{\frac{3}{2}}}{\frac{1}{2}\alpha^2\kappa^4}, \quad R = \frac{(9\kappa^2+\alpha^2)^{\frac{3}{2}}(16\kappa^2+\alpha^2)^{\frac{3}{2}}}{\frac{1}{2}\alpha^2\kappa^4}. \tag{5.10}$$

Figure 2 shows R as a function of α/κ for the first of these two odd modes of disturbance. The minimum value of R for this mode is 62.9 and occurs at $\alpha/\kappa = 0.963$, these values being given accurately by the first member of (5.10). The minimum values of R for higher-order odd modes are much larger.

Calculation of the first few Fourier coefficients (F_n) shows that the neutral first odd mode of disturbance with minimum R is an approximately square-sectioned roll cell with nested closed streamlines between the boundaries $\kappa z = p\pi$, $(p+1)\pi$ and $0.963\kappa x = q\pi$, $(q+1)\pi$ where p and q are integers, as shown in figure 3(*a*). Note that the streamlines are not exactly symmetrical about the centre of a cell. The vertical component of fluid velocity is larger in magnitude at a value of z at which $\mathrm{d}\rho_1/\mathrm{d}z > 0$ than it is at the corresponding position where $\mathrm{d}\rho_1/\mathrm{d}z$ is negative with

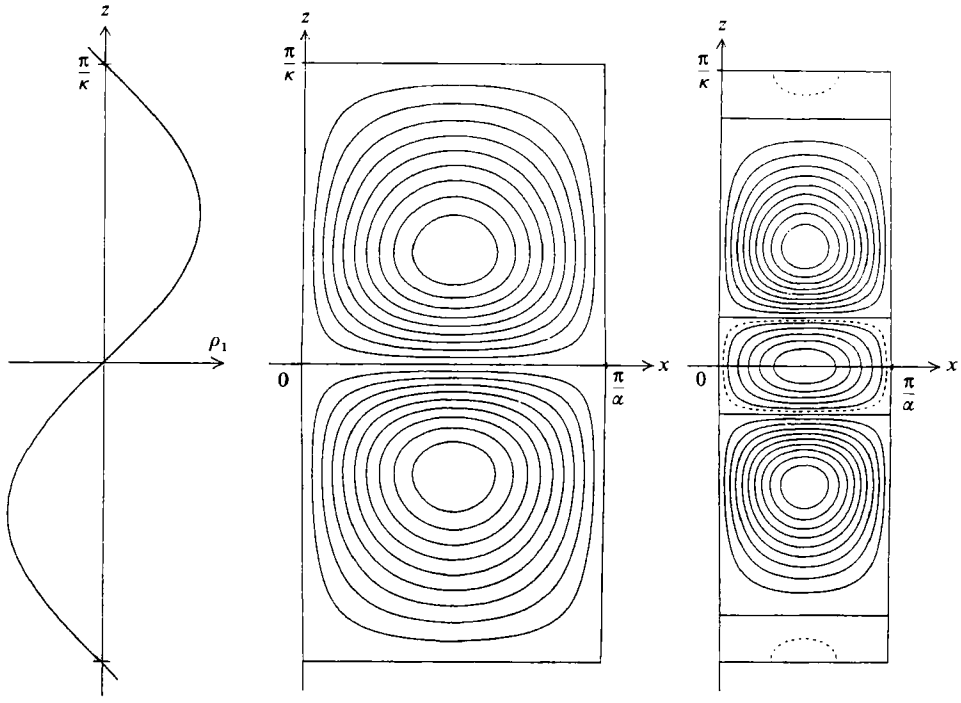

FIGURE 3. Streamlines of neutral disturbances at the minimum of R with respect to α. (*a*) The first odd mode; (*b*) the second even mode. The increments in the stream function between two adjoining continuous curves are equal. The dotted curves in (*b*) are arbitrarily chosen intermediate streamlines.

the same magnitude. This and other numerical details are consistent with the interpretation of the roll cells as being driven by the overturning of the statically unstable fluid in every alternate half-wavelength.

We saw in §3 that, when $\mathrm{d}\rho_1/\mathrm{d}z$ is constant, the value of $\mathrm{d}\rho_1/\mathrm{d}z$ at which a neutral disturbance sinusoidal with respect to both x and z can exist in unbounded fluid is given by

$$\frac{g}{\kappa^4 D\nu\rho_0}\frac{\mathrm{d}\rho_1}{\mathrm{d}z} = \frac{(\kappa^2+\alpha^2)^3}{\kappa^4\alpha^2}, \tag{5.11}$$

whereas when $\mathrm{d}\rho_1/\mathrm{d}z \propto \cos\kappa z$ a neutral odd-mode disturbance of lowest order exists at

$$R = \frac{g}{\kappa^4 D\nu\rho_0}\left(\frac{\mathrm{d}\rho_1}{\mathrm{d}z}\right)_{z=0} = \frac{(\kappa^2+\alpha^2)^{\frac{3}{2}}(4\kappa^2+\alpha^2)^{\frac{3}{2}}}{\frac{1}{2}\kappa^4\alpha^2}. \tag{5.12}$$

The minimum value of the expression (5.11) for fixed κ occurs at $\alpha/\kappa = 0.71$ and is 6.8, whereas that of (5.12) occurs at $\alpha/\kappa = 0.96$ and is 63, the latter critical density gradient being larger because in the case of the sinusoidal density profile some parts of the fluid have no tendency to overturn in a square cell.

5.2. *Disturbance modes with W even in z*

When the series of cosine terms in (5.3) is substituted for $W(z)$ in (5.2) we get

$$\sum_{n=0}^{\infty} L_n G_n \cos n\kappa z = \tfrac{1}{2}\alpha^2\kappa^4 R \sum_{n=0}^{\infty} G_n\{\cos(n-1)\,kz + \cos(n+1)\,\kappa z\}, \tag{5.13}$$

where L_n is as defined in (5.4). Equating coefficients of $\cos n\kappa z$ gives

$$\left.\begin{aligned} &L_0 G_0 = \tfrac{1}{2}\alpha^2\kappa^4 R G_1, \quad L_1 G_1 = \tfrac{1}{2}\alpha^2\kappa^4 R(2G_0 + G_2) \\ \text{and} \quad &L_n G_n = \tfrac{1}{2}\alpha^2\kappa^4 R(G_{n-1} + G_{n+1}) \quad (n = 2, 3, \ldots). \end{aligned}\right\} \tag{5.14}$$

On truncating the Fourier series at various small values of n in the same way we find for the first and second even modes of lowest order

$$\tfrac{1}{2}\alpha^2\kappa^4 R = (\tfrac{1}{2}L_0 L_1)^{\frac{1}{2}}, \quad \tfrac{1}{2}\alpha^2\kappa^4 R = (L_2 L_3)^{\frac{1}{2}} \tag{5.15}$$

respectively. The corresponding relations between R and α/κ for a neutral disturbance are then

$$R = \frac{\sqrt{2}\alpha(\kappa^2+\alpha^2)^{\frac{3}{2}}}{\kappa^4}, \quad R = \frac{(4\kappa^2+\alpha^2)^{\frac{3}{2}}(9\kappa^2+\alpha^2)^{\frac{3}{2}}}{\frac{1}{2}\alpha^2\kappa^4}, \tag{5.16}$$

and the exact values are shown graphically in figure 2. The minimum value of R for the second even mode occurs at $\alpha/\kappa = 1.70$ and is 510, which is considerably larger than the minimum value of R for the first odd mode of disturbance. This second even mode also has a cellular form, as shown in figure 3(*b*).

The first even neutral mode, however, has the surprising property of not possessing a non-zero minimum of R. The first of the relations (5.16) has the asymptotic form $R \sim \sqrt{2}\alpha/\kappa$ (indicated by the broken line in figure 2) as $\alpha/\kappa \to 0$. It appears that, however small the Rayleigh number may be, a neutral even mode of disturbance can be found by choosing a sufficiently small horizontal wavenumber. The first of the relations (5.15) shows that the rate of growth of the first even mode of disturbance at prescribed values of R, α/κ and ν/D is given approximately by

$$\left(\frac{\gamma}{D}+\alpha^2\right)\left(\frac{\gamma}{\nu}+\alpha^2\right)\left(\frac{\gamma}{D}+\kappa^2+\alpha^2\right)\left(\frac{\gamma}{\nu}+\kappa^2+\alpha^2\right) = \frac{\frac{1}{2}\alpha^2\kappa^8 R^2}{\kappa^2+\alpha^2}. \tag{5.17}$$

For the particular case $\nu/D = 1$, this equation can be solved explicitly for γ:

$$\frac{\gamma}{(\nu D)^{\frac{1}{2}}\kappa^2} = -\frac{\alpha^2}{\kappa^2} - \frac{1}{2} + \frac{1}{2}\left\{1 + \frac{2\sqrt{2}\alpha R}{(\kappa^2+\alpha^2)^{\frac{1}{2}}}\right\}^{\frac{1}{2}}, \tag{5.18}$$

the corresponding exact values being shown graphically in figure 4(*a*). The shape of the curves relating γ and α is qualitatively similar at other values of ν/D, as shown in figure 4(*b*). For any $R > 0$ there is a range of values of α/κ bounded by $\alpha/\kappa = 0$ for which $\gamma > 0$. A sinusoidal density profile is evidently always unstable.

The above theory suggests that if a sinusoidal distribution of density is suddenly set up in stationary fluid by some means, the disturbance that emerges by the familiar process of differential growth is that for which γ is a maximum with respect to α at the given value of R, and so is characterized by points lying on the broken curve in figure 4(*a*).

5.3. *The first even mode: a global type of instability*

The result that disturbances of large horizontal wavelength become unstable as soon as the Rayleigh number is made non-zero is unusual for cases of stationary stratified fluid, and we shall therefore examine the nature of the disturbance motion to see the mechanism of the instability.

It may be shown readily that for a neutral disturbance with small horizontal

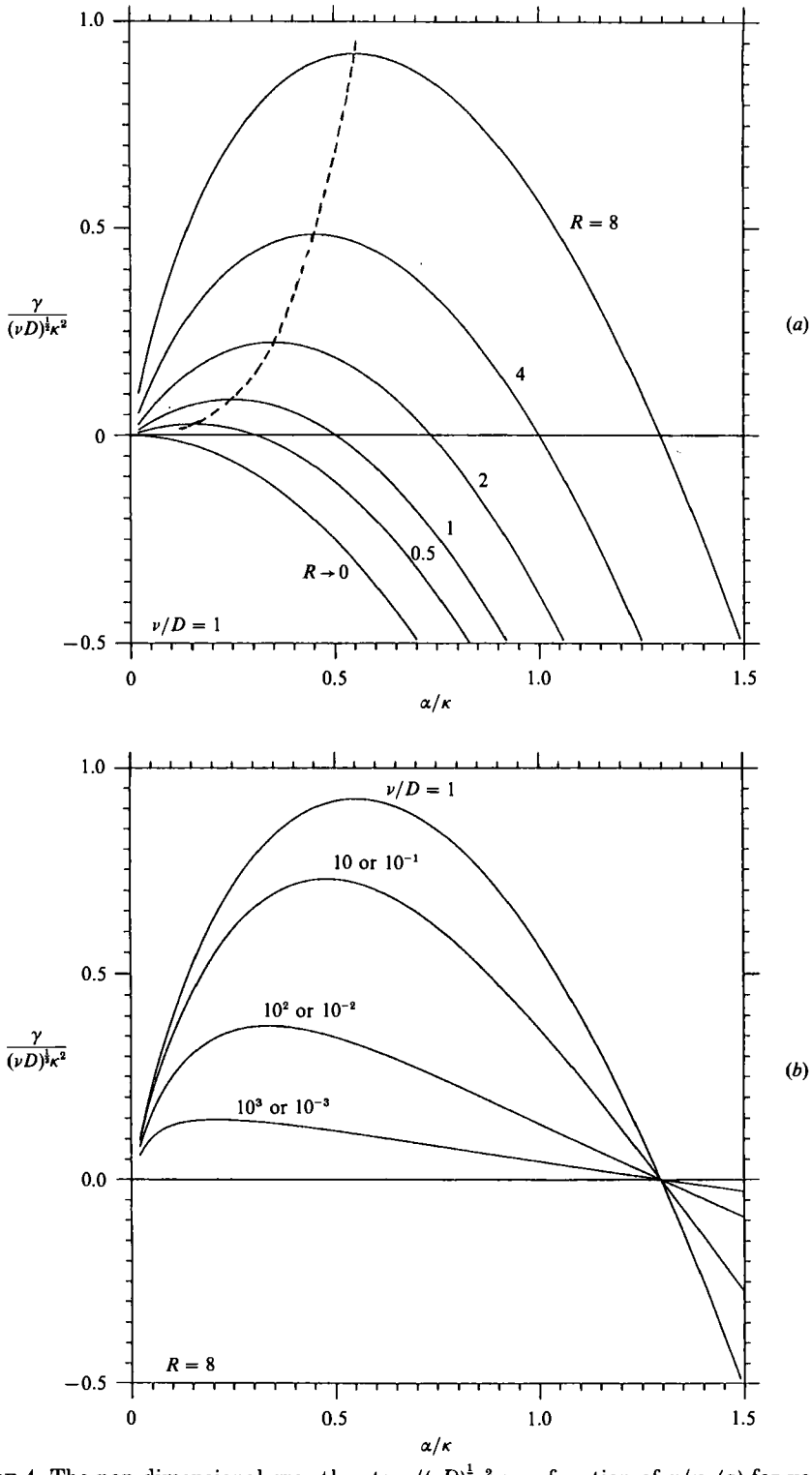

FIGURE 4. The non-dimensional growth rate $\gamma/(\nu D)^{\frac{1}{3}}\kappa^2$ as a function of α/κ, (*a*) for various values of R when $\nu/D = 1$, and (*b*) for various values of ν/D when $R = 8$; first even mode. The broken curve in (*a*) passes through the maxima of the solid curves.

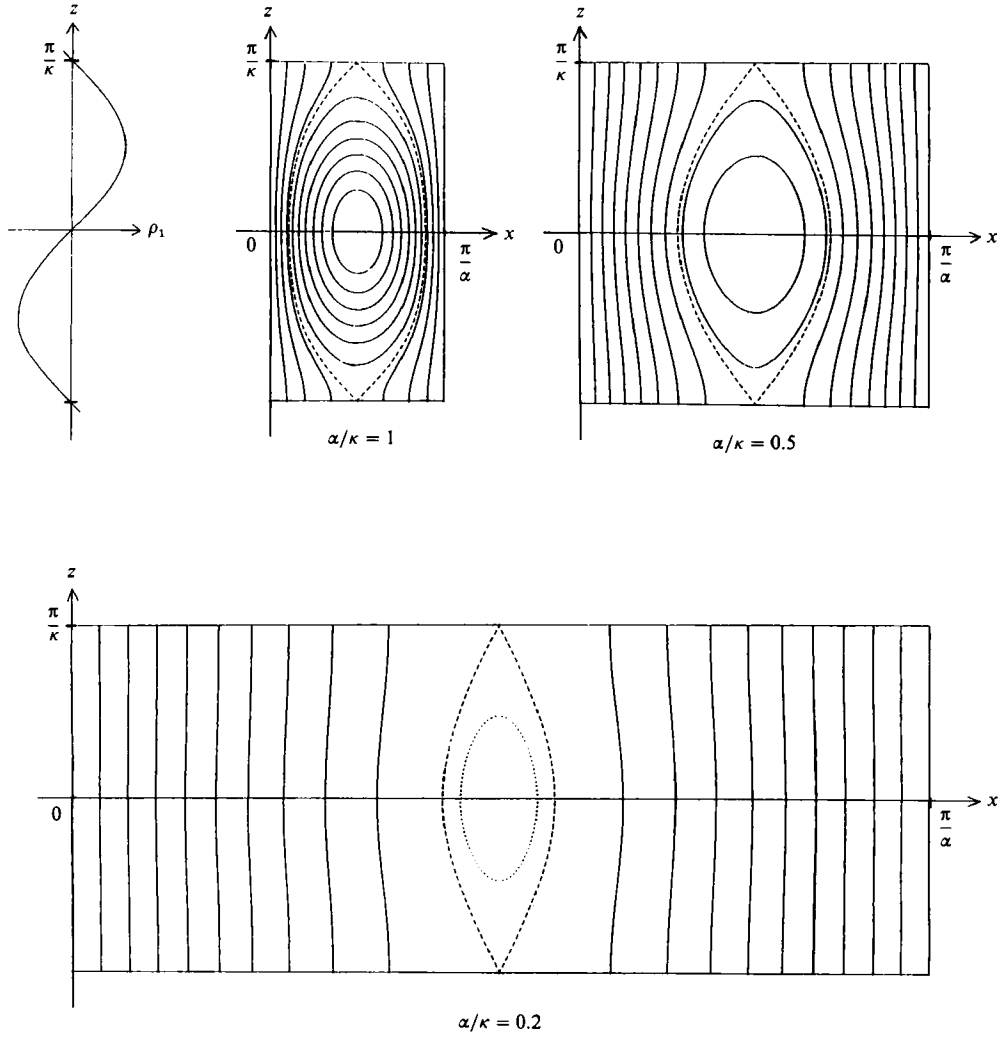

FIGURE 5. Streamlines of a neutral disturbance in the first even mode, with $\alpha/\kappa = 1, 0.5, 0.2$. The streamline pattern is periodic in x and z with periods π/α and $2\pi/\kappa$ respectively. The increments in the stream function between two adjoining continuous curves are equal. The broken curve in each diagram is the boundary of the region of closed streamlines. The dotted curve for the case $\alpha/\kappa = 0.2$ is an arbitrarily chosen closed streamline.

wavenumber the Fourier coefficients G_n given by (5.14) with the first relation in (5.16) have rapidly diminishing magnitudes; specifically

$$\frac{G_1}{G_0} = \frac{\sqrt{2}\alpha^3}{(\kappa^2+\alpha^2)^{\frac{3}{2}}}, \quad \frac{G_n}{G_0} = 0\left(\frac{\alpha^{3n}}{\kappa^{3n}}\right) \quad (n \geqslant 2).$$

Thus the approximations to the horizontal and vertical components of velocity correct to $O(\alpha^3/\kappa^3)$ are

$$u = \sqrt{2}G_0\frac{\alpha^2}{\kappa^2}\sin\alpha x \sin\kappa z, \quad w = G_0\cos\alpha x\left(1+\frac{\sqrt{2}\alpha^3}{\kappa^3}\cos\kappa z\right), \tag{5.19}$$

showing that the velocity vector is nearly vertical everywhere. This is likewise evident from the streamlines of a neutral disturbance within the region $\kappa|z| \leqslant \pi$,

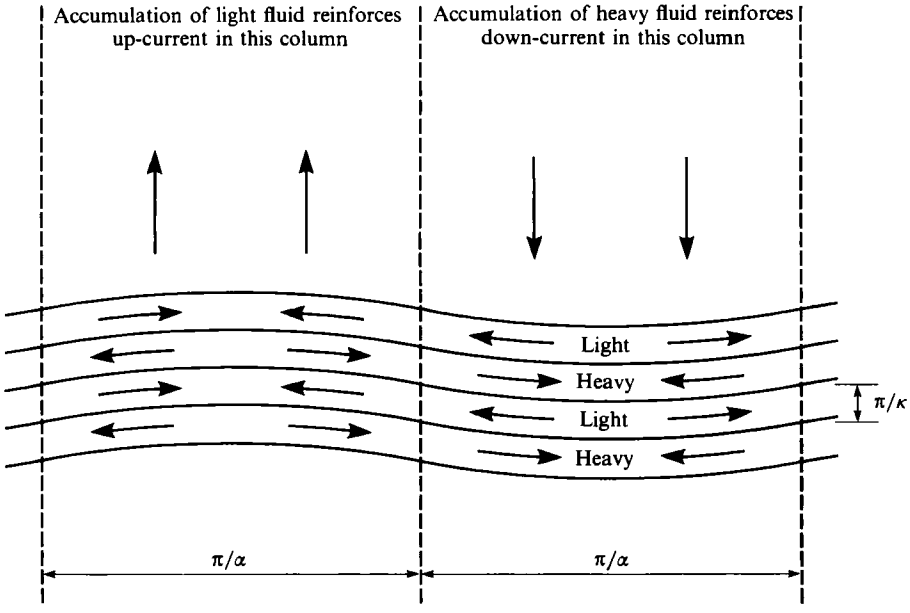

FIGURE 6. Sketch showing the vertical and horizontal components of velocity in a neutral first even global-mode disturbance to a sinusoidal density distribution; $\alpha/\kappa = 0.1$. The velocity distribution is periodic in x and z with periods $2\pi/\alpha$ and $2\pi/\kappa$ respectively.

$0 \leqslant \alpha x \leqslant \pi$ shown in figure 5 for the cases $\alpha/\kappa = 1, 0.5, 0.2$. We see also that since the slope of a material surface which is horizontal in the undisturbed state has the sign of $\partial w/\partial x$, that is, of $-\sin \alpha x$, the sign of the small horizontal component of velocity corresponds to a motion of a layer of denser fluid ($\rho_1 > 0$) *down* the slope and a motion of a layer of less dense fluid *up* the slope. Figure 6 shows these differential sliding motions of the tilted layers of fluid schematically for a neutral disturbance with $\alpha/\kappa = 0.1$. There is a tendency for heavy fluid to accumulate in the troughs of the wavy disturbance with a corresponding depletion of light fluid, and vice versa in the crests of the wave; and in the case of a neutral disturbance this tendency is balanced by the restoring effect of diffusion and the restraining effect of viscosity.

Now that we have the picture provided by figure 6, it is plausible and natural that a wavy disturbance of long horizontal wavelength which tilts the layers of stratified fluid to the horizontal should generate a relative sliding motion due to gravity which tends to separate the light and heavy fluid into different vertical compartments of width π/α and so to reinforce the initial disturbance motion. This instability mechanism is *global* in character, in contrast to the local type of instability which generates an overturning motion in roll cells with dimensions comparable with the vertical thickness of the layer of fluid in which $\mathrm{d}\rho_1/\mathrm{d}x$ is positive. A homely illustration of the mechanism is provided by a large shallow tray which is filled with water to a depth of a centimetre or two. It is difficult to pick up the tray without spilling the water because the slightest tilt to the horizontal causes the water to flow to the lowest point of the tray, where the accumulation of water depresses that end of the tray even more.

It seems likely that, as in the case of Rayleigh–Taylor instability of a horizontal interface across which there is a density jump, in the nonlinear phase of development of the growing disturbance there is an approach to a state in which falling heavy fluid

and rising light fluid occupy adjoining vertical columns or fingers of width π/α, the value of α being that for which the growth rate of a small disturbance is a maximum at the given value of R. There may not be an asymptotic steady state, however, because diffusion in the horizontal direction gradually eliminates the density variations.

It will be recalled that at the beginning of this section we anticipated the existence of solutions of the governing equation (5.2) for which $W(z)$ is periodic in z with period $2\pi/\kappa$ like the undisturbed density distribution. Floquet theory for ordinary differential equations with periodic coefficients (Ince 1944) suggests the further possibility of solutions which are periodic in z with period $2\pi N/\kappa$, where N is an integer and $N = 1$ for the 'synchronous' disturbance examined above. We have examined the first two even-mode 'subharmonic' disturbances (for which $N = 2, 3$) by the above method, and find that, although they are unstable, the Rayleigh number for a neutral disturbance does not vanish with α/κ and is larger than that for a synchronous disturbance with the same (small) value of α/κ.

However, new cases in which $N \gg 1$ prove to be interesting. Since the vertical period of the disturbance is here large compared with the period $2\pi/\kappa$, the disturbance velocity $W(z)$ is likely to be approximately uniform over one period of the undisturbed density profile, thereby reproducing the conditions for the global tilting-sliding mechanism sketched in figure 6. We do in fact find by the method used above that, when N is equal to the large ratio κ/α, the Rayleigh number for a neutral disturbance asymptotes to $4\alpha/\kappa$ as $\alpha/\kappa \to 0$. The disturbance motion here occupies a large rectangular cell with both linear dimensions of order $2\pi/\alpha$, and the vertical component of the disturbance velocity is consequently weak over some parts of the cell. An even more unstable disturbance is therefore obtained by choosing

$$N \gg \kappa/\alpha \gg 1, \tag{5.20}$$

because now the disturbance cell is much larger in the vertical than in the horizontal direction and the tilting of the layers of heavier and lighter fluid is exactly as found for the first even synchronous mode when $\alpha/\kappa \ll 1$ (see figures 5 and 6). Again we have confirmed this analytically, and find $\sqrt{2}\alpha/\kappa$ for the Rayleigh number of a neutral disturbance satisfying the conditions (5.20). For any large values of N and of κ/α we obtain the expression

$$R = \frac{\sqrt{2}\alpha}{\kappa}\left(1 + \frac{\kappa^2}{N^2\alpha^2}\right)^{\frac{3}{2}} \tag{5.21}$$

for the Rayleigh number of a neutral disturbance.

In summary, all subharmonics, whether even or odd, have a cellular structure because the first term in the Fourier series representing $W(z)$ is not constant. The ratio of the vertical to horizontal dimensions of the cell is $N\alpha/\kappa$, and only when this ratio is large can the global tilting-sliding mechanism operate effectively. As $N\alpha/\kappa \to \infty$, and provided $\alpha/\kappa \ll 1$, the relation between $\gamma/(\nu D)^{\frac{1}{2}}\kappa^2$, R, ν/D and α/κ, for both even- and odd-mode subharmonics, tends to that already found for the first even-mode synchronous disturbance, which remains the most unstable type.

6. Fluid with zero density gradient outside a central layer

The analysis of the preceding section for a sinusoidal undisturbed density variation led to the identification of a global type of instability characterized by the feature that the Rayleigh number for neutral stability tends to zero as the horizontal

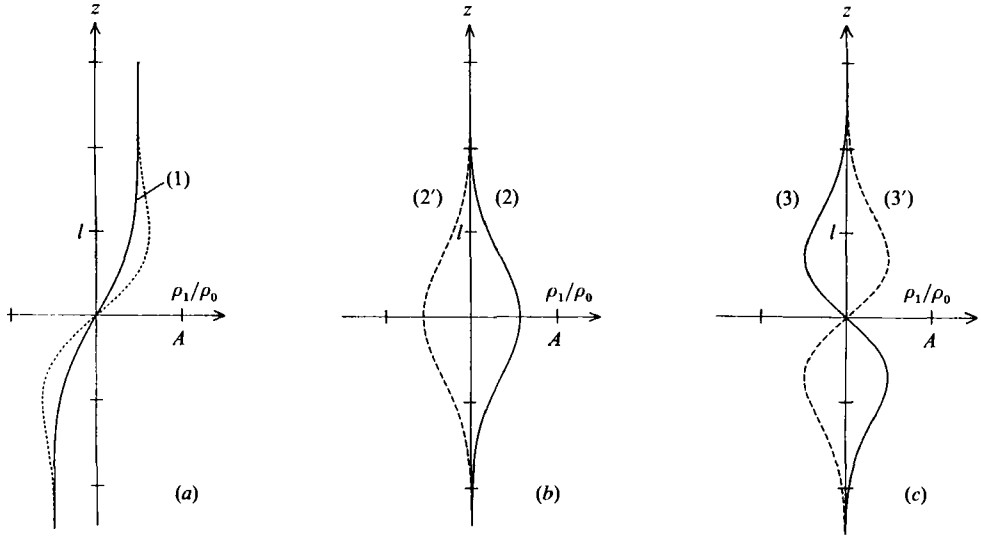

FIGURE 7. Types of density stratification with zero gradient outside a central layer of thickness l.

wavelength becomes large. Now that the basic mechanism for the instability has been explained, it is worthwhile to enquire whether there are other density profiles for which similar instabilities exist.

The results for a sinusoidal density profile suggest consideration of fluid with non-uniform density in a single central horizontal layer, since here too heavy or light fluid would slide laterally when the layer is tilted. Figure 7 shows schematically three types of undisturbed density stratification which may conveniently be considered together. These three are (1) a layer of transition from light fluid below to heavy fluid above, (2, 2′) an isolated layer of heavy or light fluid, and (3, 3′) a heavy and a light sub-layer one on top of the other. Here, 'heavy' and 'light' mean relative to the base density ρ_0. In each of these three cases a layer with thickness of $O(l)$ in which the density is non-uniform is sandwiched between two semi-infinite expanses of fluid in which the density gradient tends rapidly to zero. Our three cases differ significantly from density profiles studied previously within the context of penetrative convection (§4) inasmuch as the fluid is not statically stable outside the central layer. As a consequence, we shall again find that the fluid is unstable to disturbances with long horizontal wavelengths at small values of the Rayleigh number. In case (1), which is the Rayleigh–Taylor type of instability with effects of buoyancy diffusion included, the disturbances do not exhibit the novel tangential sliding of fluid layers that we found for a sinusoidal density profile, but we include consideration of case (1) in view of its close mathematical connection with cases (2) and (3).

6.1. *Asymptotic analysis for* $\alpha l \ll 1$

Our starting point is equation (2.11). Fourier transformation of both sides yields the following expression for the transform of $W(z)$:

$$\hat{W}(\omega) = \mathscr{F}[W(z)] = \frac{g\alpha^2/(\nu D)}{(\omega^2+\alpha^2+\gamma/D)(\omega^2+\alpha^2+\gamma/\nu)(\omega^2+\alpha^2)} \int_{-\infty}^{\infty} \frac{1}{\rho_0}\frac{\mathrm{d}\rho_1}{\mathrm{d}z} W(z)\, \mathrm{e}^{\mathrm{i}\omega z}\, \mathrm{d}z. \tag{6.1}$$

In general, (6.1) leads via the convolution theorem to an integral equation for $\hat{W}(\omega)$ which seems not to be simpler than the original differential equation (2.11). However, we are interested primarily in the asymptotic behaviour of W when $\alpha l \ll 1$, and an approximate approach starting directly from (6.1) enables us to identify – without having to assume any specific functional forms for ρ_1 – the key parameters of the three types of density profile that determine their stability properties. Since the undisturbed density gradient $\mathrm{d}\rho_1/\mathrm{d}z$ goes to zero outside the central layer, the value of the integral in (6.1) is determined approximately by the behaviour of $W(z)$ near $z = 0$. We therefore form a Taylor expansion of $W(z)\exp(\mathrm{i}\omega z)$ about $z = 0$, and evaluate this integral as

$$\int_{-\infty}^{\infty} \frac{1}{\rho_0}\frac{\mathrm{d}\rho_1}{\mathrm{d}z} W(z)\,\mathrm{e}^{\mathrm{i}\omega z}\,\mathrm{d}z = \sum_{n=0}^{\infty} \frac{M_n}{n!}\left[\frac{\mathrm{d}^n(W\,\mathrm{e}^{\mathrm{i}\omega z})}{\mathrm{d}z^n}\right]_{z=0}, \tag{6.2}$$

where

$$M_n = \int_{-\infty}^{\infty} z^n \frac{1}{\rho_0}\frac{\mathrm{d}\rho_1}{\mathrm{d}z}\,\mathrm{d}z. \tag{6.3}$$

The formal expansion procedure is predicated upon the expectation that the vertical component of velocity varies slowly over the central layer when $\alpha l \ll 1$, this being suggested by experience with the sinusoidal case, where the velocity for the global mode at long horizontal wavelengths varied very little with z despite periodic variations in $\mathrm{d}\rho_1/\mathrm{d}z$.

Equations (6.1) and (6.2) together give rise to functions of ω having the form

$$\hat{f}_k(\omega) = \frac{(\mathrm{i}\omega)^k}{(\omega^2+\alpha^2+\gamma/D)(\omega^2+\alpha^2+\gamma/\nu)(\omega^2+\alpha^2)}.$$

Inversion requires use of the following identity, derivable by contour integration techniques:

$$f_k(z) = \mathscr{F}^{-1}[\hat{f}_k(\omega)] = \frac{(\pm 1)^k \alpha^{k-1}\nu^2}{2\gamma^2}\left[\frac{\mathrm{e}^{\mp\alpha z}}{P} + \frac{\sigma_1^{k-1}\,\mathrm{e}^{\mp\sigma_1\alpha z}}{1-P} + \frac{\sigma_2^{k-1}\,\mathrm{e}^{\mp\sigma_2\alpha z}}{P(P-1)}\right] \quad (z \gtrless 0), \tag{6.4}$$

where

$$\sigma_1 = \left(1+\frac{\gamma}{\alpha^2\nu}\right)^{\frac{1}{2}}, \quad \sigma_2 = \left(1+\frac{\gamma}{\alpha^2 D}\right)^{\frac{1}{2}},$$

and P is the Prandtl number ν/D. (Contrary to appearances the expression (6.4) is not singular at $P = 1$ nor at $\gamma = 0$.) We note for future use that for a neutral disturbance ($\gamma = 0$), (6.4) assumes the limiting form

$$f_k(z) = \frac{(\pm 1)^k \alpha^{k-5}}{16}[(k-1)(k-3) \mp (2k-3)\alpha z + (\alpha z)^2]\,\mathrm{e}^{\mp\alpha z} \quad (z \gtrless 0). \tag{6.5}$$

In terms of the functions f_k given by (6.4), the inversion of (6.1) leads to

$$W(z) = \frac{g\alpha^2}{\nu D}\{M_0 W(0) f_0 + M_1[W'(0)f_0 + W(0)f_1] + \tfrac{1}{2}M_2[W''(0)f_0 + 2W'(0)f_1 + W(0)f_2] + \ldots\}, \tag{6.6}$$

where the prime denotes differentiation with respect to z. Equation (6.6) specifies $W(z)$ in terms of the values of W and its derivatives at $z = 0$, moments of the undisturbed density gradient $\mathrm{d}\rho_1/\mathrm{d}z$, and the known functions $f_k(z)$. As is evident

from (6.4), the $f_k(z)$ generally decay exponentially on the spatial scales α^{-1}, $(\alpha\sigma_1)^{-1}$ and $(\alpha\sigma_2)^{-1}$. Consistency of the asymptotic analysis requires that all these lengths be much larger than the thickness of the central layer. Thus, in addition to $\alpha l \ll 1$, further *a posteriori* conditions for validity of the approximate approach are $\gamma \ll \nu/l^2$ and $\gamma \ll D/l^2$. The latter two inequalities require the timescale of growth to be much larger than the times for momentum and buoyancy diffusion over a distance equal to the central layer thickness. It may be deduced from subsequent results that a sufficient condition for satisfaction of all three inequalities is smallness of the Rayleigh number based on the layer thickness.

It may be noted in passing that, although we are ignoring possible effects of time evolution of the base density profile $\rho_0+\rho_1$ due to diffusion, our asymptotic analysis indicates that such temporal changes have *no* effect to leading order at large horizontal wavelengths. A conserved quantity governed by the diffusion equation evolves in such a way that the moments M_0 and M_1 of the spatial gradient are constant, and so too is M_2 when $M_0 = 0$. The growth rate γ is determined asymptotically by $\rho_0+\rho_1$ only through its dependence upon these moments (in a manner to be detailed below), all of which are unaffected by diffusive spreading of the base profile. The only restriction is that the time be not so long that the broadening central layer ceases to be thin compared with the horizontal wavelength.

Case (1): *a transition between two different densities*

The zeroth-order moment (see (6.3)) specifies the fractional change in density:

$$M_0 = \frac{\rho_1|_{z\to\infty} - \rho_1|_{z\to-\infty}}{\rho_0}.$$

At the lowest order of approximation, equation (6.6) gives for $W(z)$ the expression

$$W(z) \sim \frac{g\alpha^2 M_0}{\nu D} W(0) f_0(z). \tag{6.7}$$

The validity of this expression for $W(z)$ at $z = 0$ requires that

$$\frac{g\alpha^2 M_0}{\nu D} \sim \frac{1}{f_0(0)}. \tag{6.8}$$

For the special case of a neutrally stable disturbance (see (6.5)) these expressions become

$$R = \frac{gl^3 M_0}{\nu D} \sim \frac{16}{3}(\alpha l)^3 \tag{6.9}$$

and

$$W(z) \sim W(0)\,\mathrm{e}^{-|\alpha z|}[1 + |\alpha z| + \tfrac{1}{3}(\alpha z)^2]. \tag{6.10}$$

The flow field given by (6.10) is illustrated in figure 8(*a*), and consists of rolls which decay exponentially with z on the scale α^{-1}. The essentially vertical flow near $z = 0$ is like that for the sinusoidal case. Likewise the Rayleigh number for neutral stability tends to zero as $\alpha l \to 0$, although now with the third (not the first) power of αl. It is understandable that the damping effects of viscous stresses and diffusion should be more important for interleaved layers of heavy and light fluid than for a configuration where the heavy fluid is separated from the light fluid. We shall see in §7 that the growth rate γ is proportional to the *same* power of α in the sinusoidal case and in case (1) when diffusion and viscous effects are absent.

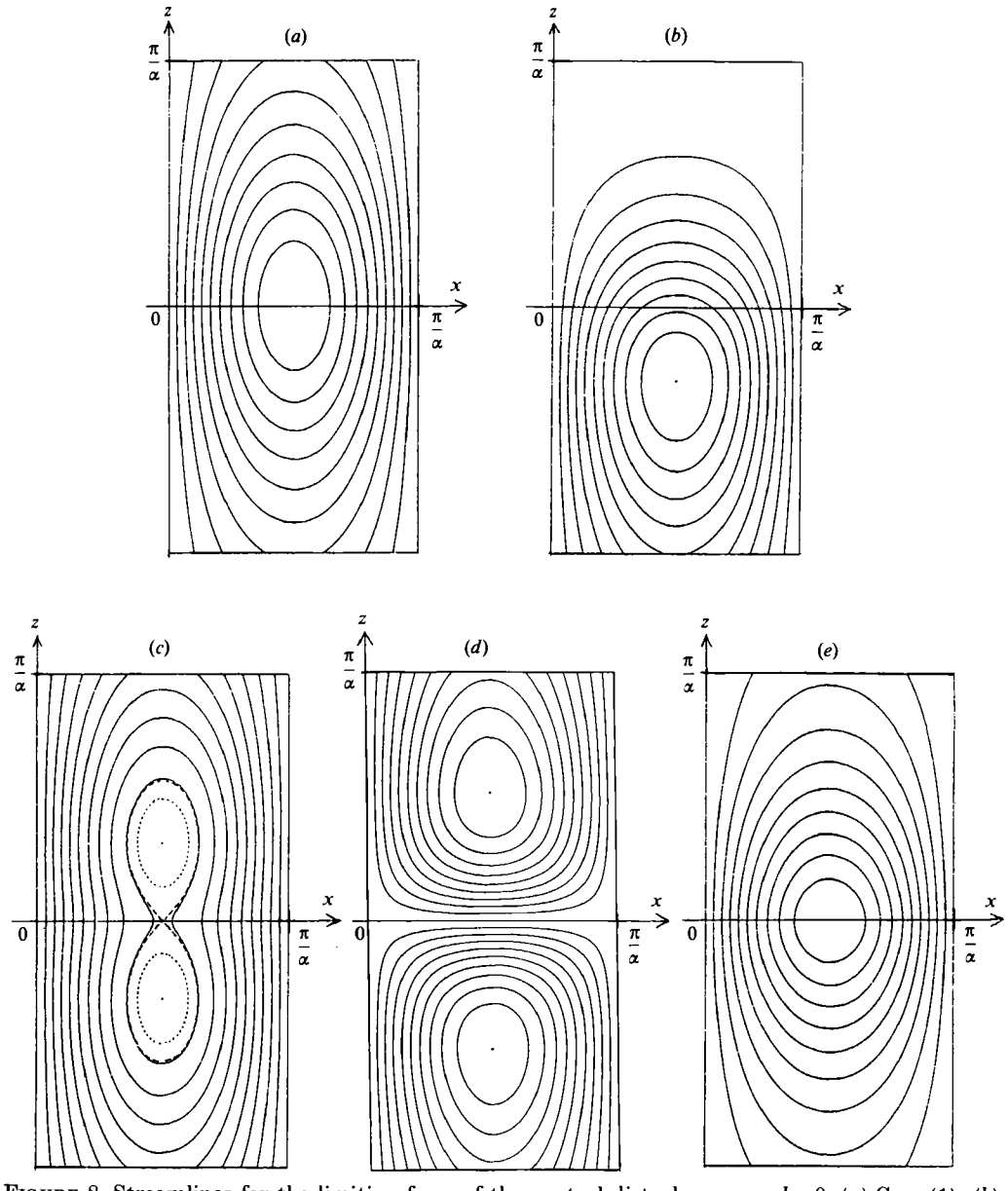

FIGURE 8. Streamlines for the limiting form of the neutral disturbance as $\alpha l \to 0$. (*a*) Case (1); (*b*) case (2); (*c*) case (3), even mode; (*d*) case (3), odd mode; (*e*) case (3′). The increments in the stream function between two adjoining continuous curves are equal. The broken curve in (*c*) is the boundary of two inner regions of closed streamlines, and the dotted curves are arbitrarily chosen intermediate streamlines.

Equation (6.6) makes it clear that the asymptotic relations (6.7)–(6.10) derive purely from the existence of a density difference. Details of the transition from light to heavy fluid do not enter at lowest order, provided only that the horizontal wavelength is much larger than the thickness of this central layer. The succeeding terms in (6.6) represent higher-order corrections to the leading asymptotic behaviour, and are affected by the specific form of the undisturbed density gradient through

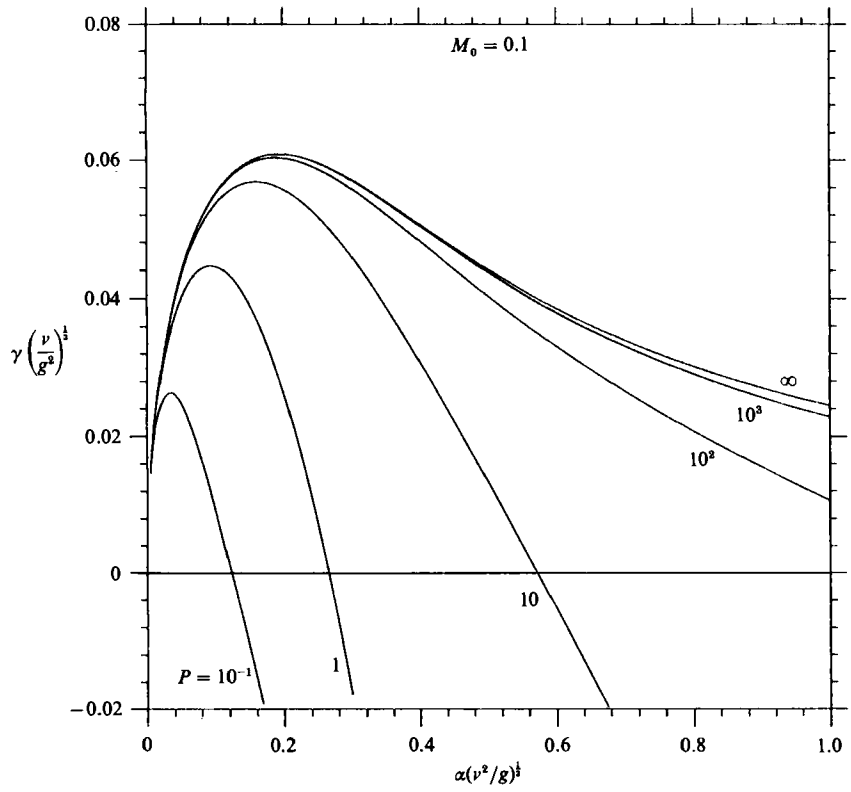

FIGURE 9. Growth rate γ as a function of the horizontal wavenumber α for density variations of type (1) in the limit as $\alpha l \to 0$. In this limit the central layer is characterized solely by the fractional density difference M_0, here equal to 0.1 for all the curves.

their dependence upon its higher moments, as will be demonstrated later. If ρ_1 is not an odd function of z (e.g. when $M_1 \neq 0$), then higher-order corrections will cause small deviations from the symmetry of the leading-order flow about the central plane $z = 0$. It is worth noting that, at lowest order, the density gradient $\mathrm{d}\rho_1/\mathrm{d}z$ acts as a Dirac delta function in (6.1), picking out the value of $W(z)\exp(\mathrm{i}\omega z)$ at $z = 0$.

When $\alpha l \ll 1$ the central layer looks infinitesimally thin on the scale α^{-1} of spatial variations in the disturbance flow, and case (1) is then a body of heavy fluid lying above a body of light fluid separated from it by an interface. This situation was addressed by Taylor (1950) for the case of inviscid flow with surface tension at the interface, and his work was later extended by others (Bellman & Pennington 1954; see also Chandrasekhar 1961) to include the effects of fluid viscosity with or without interfacial tension. Our analysis makes a small new contribution to this classical problem inasmuch as our results show the effect of the diffusion of buoyancy on a disturbance in the absence of interfacial tension. Figure 9 shows the dependence of the growth rate γ, calculated numerically from (6.8) and (6.4), on the horizontal wavenumber α for a fixed value of the fractional density difference M_0 and various values of ν/D. Here we have used the characteristic length $(\nu^2/g)^{\frac{1}{3}}$ and the kinematic viscosity ν to make γ and α dimensionless, as in Chandrasekhar (1961). The limiting functional relation as $\nu/D \to \infty$ is numerically identical with that given by Chandrasekhar for the case where the fluid has viscosity but no surface tension and no diffusion of buoyancy. The curves corresponding to different values of ν/D

indicate that diffusion of buoyancy inhibits the growth of disturbances and makes possible a condition of neutral stability. In this respect diffusion has the same additional effect as surface tension, although the operative physical mechanisms are quite different. For an interface with surface tension, the neutral disturbance corresponds to stationary fluid and a deformation of the interface which prevents the further release of potential energy by fingering of heavy fluid down into light fluid and vice versa. In our situation the neutrally stable disturbance involves a steady flow, and the 'interface' (central transition layer) remains stationary because the density now diffuses relative to the fluid and fluid may pass through the 'interface' without carrying it along.

All the curves in figure 9 have the asymptotic behaviour $\gamma^2 \sim \frac{1}{2}g\alpha M_0$ as α becomes small. This is the relation derived by Taylor (1950) for the inviscid (and non-diffusive) case.

Case (2): *a layer of either heavy or light fluid*

Here the values of the undisturbed density far above and below the central layer are identical, whence the first term on the right-hand side of (6.6) vanishes. The value of

$$-M_1 = \int_{-\infty}^{\infty} \frac{\rho_1}{\rho_0} \mathrm{d}z,$$

representing the excess mass per unit area of the layer divided by ρ_0, now determines at leading order whether the stratified fluid is dynamically stable. Equation (6.6) specifies $W(z)$ in terms of the values of W and W' at $z = 0$, and leads to two linear equations in the variables $W(0)$ and $W'(0)$ which determine M_1 in terms of α and γ (and P) as an eigenvalue:

$$\frac{g\alpha^2|M_1|}{\nu D} \sim \{f_0(0)f'_1(0)\}^{-\frac{1}{3}}. \tag{6.11}$$

This expression is applicable for either sign of M_1.

For a neutrally stable disturbance, we have

$$R = \frac{gl^2|M_1|}{\nu D} \sim \frac{16}{\sqrt{3}}(\alpha l)^2. \tag{6.12}$$

The corresponding flow for case (2), given by

$$W(z) \sim W(0)\,\mathrm{e}^{-|\alpha z|}\left[1 + \left(|\alpha z| - \frac{\alpha z}{\sqrt{3}}\right)\left(1 - \frac{\alpha z}{\sqrt{3}}\right)\right], \tag{6.13}$$

is now asymmetric, the rolls having centres at $\alpha z \approx -0.941$, as shown in figure 8(*b*). The flow field for case (2′) is the same except reflected in the plane at $z = 0$. As before, the details of the density distribution in the central layer are of no consequence to the leading asymptotic behaviour of the global mode, which now depends only upon the moment M_1. At lowest order, the density gradient $\mathrm{d}\rho_1/\mathrm{d}z$ is effectively the derivative δ' of a Dirac delta function, picking out the derivative of $W\exp(\mathrm{i}\omega z)$ at $z = 0$ in (6.1).

Figure 10(*a*) shows the dependence of the growth rate γ upon the horizontal wavenumber α for fixed values of M_1 (such that $\alpha l \ll 1$) and $\nu/D = 1$. As in case (1), these curves derived from (6.11) and (6.4) correspond to the central layer acting as

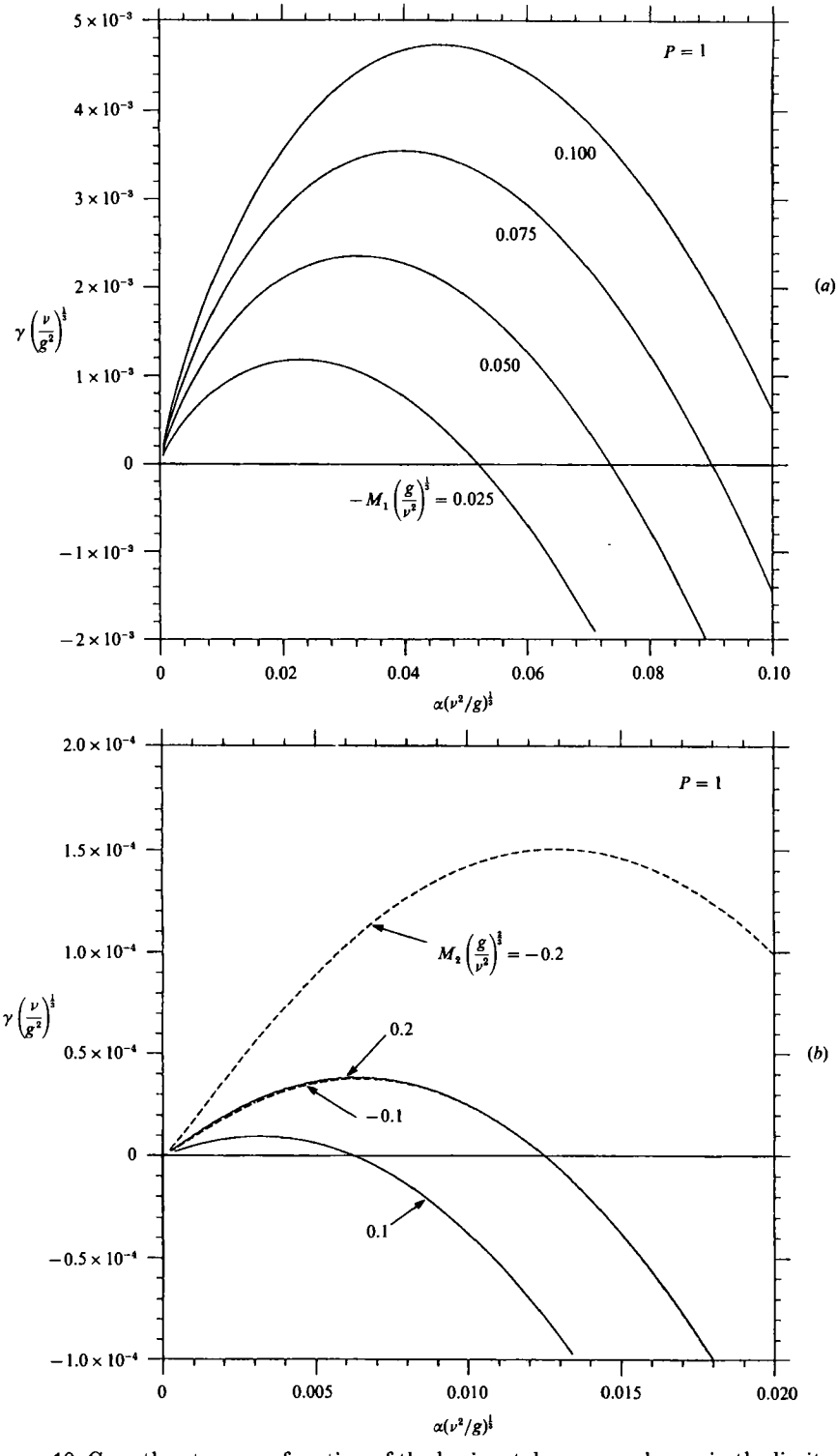

FIGURE 10. Growth rate γ as a function of the horizontal wavenumber α, in the limit $\alpha l \to 0$, (*a*) for density variations of type (2) characterized by the parameter $M_1(g/\nu^2)^{\frac{1}{3}}$, and (*b*) for types (3), even mode, (continuous curves) and (3′) (broken curves) characterized by $M_2(g/\nu^2)^{\frac{2}{3}}$; $P = 1$. Curves for type (3), odd mode, are quantitatively very similar to those for the even mode.

an infinitesimally thin interface, now characterized by the parameter M_1. It can be shown from (6.11) and (6.4) that, for each curve, γ becomes proportional to $\alpha^{\frac{6}{7}}$ as $\alpha \to 0$. This power law cannot be expressed in terms of non-dimensional variables without involving ν and D. Thus, the behaviour of the curves very near the origin does not describe the inviscid and non-diffusive limit, unlike the Rayleigh–Taylor instability (case 1). We take up the inviscid, non-diffusive limit via a different type of analysis in § 7.

Case (3): *a layer containing heavy and light fluid equally*

Density stratifications of type (3) are ones for which the density approaches the same value above and below the central layer, and for which this layer possesses zero net excess mass. The first two terms on the right-hand side of (6.6) thus vanish. The integral

$$-\tfrac{1}{2}M_2 = \int_{-\infty}^{\infty} z\frac{\rho_1}{\rho_0}\,\mathrm{d}z,$$

representing the first moment of interfacial excess mass per unit area divided by ρ_0, now determines the dynamic stability of the stratified fluid. Equation (6.6) leads to a homogeneous system of three linear equations in the quantities $W(0)$, $W'(0)$ and $W''(0)$, for which the moment M_2 represents an eigenvalue. Straightforward calculations lead to the expressions

$$\frac{g\alpha^2 M_2}{\nu D} \sim \frac{2}{f_2(0)+\{f_0(0)f_2''(0)\}^{\frac{1}{2}}},\quad \frac{1}{f_1'(0)},\quad \frac{2}{f_2(0)-\{f_0(0)f_2''(0)\}^{\frac{1}{2}}}, \tag{6.14}$$

where the first two refer to case (3), for which $M_2 > 0$ (i.e. light fluid above the heavy fluid), and the last refers to case (3′), for which $M_2 < 0$ (i.e. light fluid below the heavy fluid).

For a state of neutral stability, the two modes for case (3) lead to the same asymptotic dependence of the Rayleigh number on the horizontal wavenumber, viz.

$$R = \frac{glM_2}{\nu D} \sim 16\alpha l. \tag{6.15}$$

The corresponding flows, given by

$$W(z) \sim W(0)\{1+|\alpha z|+(\alpha z)^2\}\,\mathrm{e}^{-|\alpha z|},\quad W(z) \sim W'(0)z(1+|\alpha z|)\,\mathrm{e}^{-|\alpha z|}, \tag{6.16}$$

are illustrated in figure 8 (*c* and *d*).

The first mode is even and corresponds to the global instability mechanism described above, with the difference in detail that there are now separate cells above and below that merge into peanut-shaped rolls. The second mode is odd and shows a new type of global instability that operates by a mechanism entirely different from the tilting-sliding process characterizing the disturbances discussed previously. The new mechanism can be understood by examining the streamline pattern in figure 8 (*d*). On the scale of the diagram, the central layer is infinitesimally thin and coincident with the horizontal x-axis. The flow strips off light fluid from the upper part of the central layer, just above the axis, and carries it at first horizontally and later upwards, and likewise strips off the heavy fluid just below the axis and carries it downwards. In this mechanism there is no tendency for the central layer to deform. Instead, potential energy is released in the half-spaces $z \gtrless 0$ separately.

Neutral stability for case (3′), for which M_2 is negative, is characterized by

$$R = -\frac{glM_2}{\nu D} \sim 8\alpha l. \tag{6.17}$$

As shown in figure 8(*d*), the disturbance flow,

$$W(z) \sim W(0)(1+|\alpha z|)\,\mathrm{e}^{-|\alpha z|}, \tag{6.18}$$

is qualitatively the same as in case (1) and corresponds to the tilting-sliding mechanism.

The flows for cases (3) and (3′) correspond to a $\pm\delta''$ distribution for $\mathrm{d}\rho_1/\mathrm{d}z$. The Rayleigh number for neutral stability goes to zero with the first power of α, as in the sinusoidal case. For the even modes this is not surprising, since the density stratifications of types (3) and (3′) each contain one heavy and one light layer and therefore comprise an isolated period of the sinusoidal profile. The stripping mechanism represented by the odd mode is evidently as efficient in releasing potential energy as the tilting-sliding mechanism.

Figure 10(*b*) shows the functional dependence of the growth rate γ on the horizontal wavenumber α for the case (3) even modes, for fixed values of M_2 and $\nu/D = 1$, determined numerically from (6.14) and (6.4). As in case (2), the behaviour of the curves very near the origin, where γ is now proportional to $\alpha^{\frac{3}{5}}$, does not describe the inviscid, non-diffusive limit.

The fact that the preceding asymptotic formulae give W as a function involving $|z|$ indicates the existence of a singularity buried within our approximate scheme. Direct computation for case (1) shows that W and its first four derivatives, as given by (6.7) or (6.10), are continuous at $z = 0$, but that $\mathrm{d}^5W/\mathrm{d}z^5$ suffers a jump. In cases (2) and (3), $\mathrm{d}^4W/\mathrm{d}z^4$ and $\mathrm{d}^3W/\mathrm{d}z^3$ respectively suffer jumps. These observations, which are consistent with the interpretations of the density gradients $\mathrm{d}\rho_1/\mathrm{d}z$ in terms of the delta function, indicate that corrections to the leading asymptotic behaviour of $W(z)$ begin, at a certain order, to exhibit structure on the small spatial scale of the central layer thickness l. This is as it was in the sinusoidal case (cf. equation (5.19)), where the leading term for $W(z)$ was independent of z, but the first correction term was periodic with period $2\pi/\kappa$. Thus, the regular expansion procedure embodied in (6.2) cannot be carried out to arbitrarily many terms. Equation (6.2) should be regarded as a finite sum, where we terminate the Taylor expansion with a remainder after the last term for which the derivatives of W involved are continuous.

Appreciable thickness of the central layer

The preceding leading-order asymptotic formulae apply when the thickness of the central layer is negligible in comparison with the horizontal wavelength. Thus, l does not appear explicitly, and, as is evident from the dimensionless relations in figure 10, is present only in the interface parameters M_1 and M_2. It is of interest to improve the approximation scheme by calculating corrections to the leading behaviour, and thereby to ascertain the dynamical consequences of finite l. Here we focus upon neutral disturbances for illustrative purposes.

In order to derive a refined approximation for the Rayleigh number R in case (1), we retain all the displayed terms on the right-hand side of (6.6), and substitute for R the following expansion in powers of αl:

$$R \sim \tfrac{16}{3}(\alpha l)^3[1 + r_1(\alpha l) + r_2(\alpha l)^2],$$

in which the values of the coefficients r_1 and r_2 are to be determined. We similarly introduce

$$W'(0) \sim \mathscr{W}'_0 + \mathscr{W}'_1 \alpha l, \quad W''(0) \sim \mathscr{W}''_0,$$

where $\mathscr{W}'_0, \mathscr{W}'_1, \mathscr{W}''_0$ are coefficients and the lowest-order terms are already known from (6.10). Upon collecting terms multiplied by like powers of αl, (6.6) becomes

$$\begin{aligned}\frac{3W(z)}{16W(0)} \sim F_0(z) + (\alpha l)\left\{\frac{M_1}{M_0 l}\left[\frac{\mathscr{W}'_0}{\alpha W(0)}F_0(z) + F_1(z)\right] + r_1 F_0(z)\right\} \\ + (\alpha l)^2\left\{\frac{M_2}{2M_0 l^2}\left[\frac{\mathscr{W}''_0}{\alpha^2 W(0)}F_0(z) + 2\frac{\mathscr{W}'_0}{\alpha W(0)}F_1(z) + F_2(z)\right]\right. \\ \left. + \frac{M_1}{M_0 l}\left[\frac{\mathscr{W}'_1 + r_1 \mathscr{W}'_0}{\alpha W(0)}F_0(z) + r_1 F_1(z)\right] + r_2 F_0(z)\right\},\end{aligned} \tag{6.19}$$

where M_1 and M_2 are now defined solely by (6.3) (since the moments of ρ_1/ρ_0 do not exist when $M_0 \neq 0$) and we have put $F_k(z) = \alpha^{5-k} f_k(z)$ for brevity. It is evident from (6.3) that the ratios $M_1/M_0 l$ and $M_2/M_0 l^2$ represent $O(1)$ numbers. Validity of (6.19) at $z = 0$ confirms the leading behaviour (6.9) and requires that the coefficients multiplying αl and $(\alpha l)^2$ vanish. This leads to the conclusion that $r_1 = 0$, and gives an expression for r_2 in terms of various quantities, all of which are known except for $\mathscr{W}'_1$. The latter is found by differentiating (6.19) with respect to z. In this way, it can be shown that the Rayleigh number for case (1) possesses the asymptotic behaviour

$$R \sim \tfrac{16}{3}(\alpha l)^3\left\{1 + \frac{(\alpha l)^2}{3}\left[\frac{M_2}{M_0 l^2} - \left(\frac{M_1}{M_0 l}\right)^2\right]\right\}. \tag{6.20}$$

It is seen from (6.20) that non-zero values of M_1 of either sign decrease the Rayleigh number for neutral stability. This is expected, because non-zero M_1 is the cause of instability in cases (2) and (2′), and so here represents a destabilizing factor, albeit weaker than the dominant density jump.

For a density variation that is odd in z, like either of the two curves in figure 7(*a*), $M_1 = 0$. If the density increases monotonically with z (as illustrated by the continuous curve), then $M_2 > 0$, implying that increase of the thickness of a central layer in which there is a simple smooth transition between the two different densities at $|z| \to \infty$ has a stabilizing influence, as is generally to be expected. On the other hand $M_2 < 0$ for profiles like the dotted curve in figure 7(*a*), and here there is a destabilizing influence. This is essentially because the differential sliding motions of the different parts of the central layer go *with* the bulk motion of the two semi-infinite regions when $M_2 < 0$ whereas when $M_2 > 0$ they go *against* them.

Similar arguments yield for case (2)

$$R \sim \frac{16}{\sqrt{3}}(\alpha l)^2\left[1 + (\alpha l)^2\frac{2M_3}{3M_1 l^2}\right] \tag{6.21}$$

when ρ_1 is an even function of z, so that, in particular, $M_2 = 0$. For each of the two density distributions shown in figure 7(*b*), M_1 and M_3 have the same sign and non-zero values of l again have a stabilizing influence.

The leading-order approximations (6.15) and (6.17) for cases (3) and (3′) cannot be improved by the present regular expansion scheme, because calculation of the first correction term would involve derivatives of W possessing singular behaviour, as observed above.

6.2. *Some exact results for special density profiles of types* (2) *and* (3)

The preceding asymptotic analysis for long wavelengths and small growth rates has established forms of global disturbance to which the various stratifications are highly unstable, and it has shown that at various orders in αl these disturbances are governed asymptotically only by certain moments of the undisturbed density gradient. For arbitrary values of the parameters the stability properties will of course be influenced by the precise nature of the density stratification, and it would be useful to have some more general results, not restricted to small values of α and γ, for representative profiles. In the present subsection we consider density distributions in cases (2) and (3) such that ρ_1 is piecewise constant, for which (2.11) can be solved exactly. Although such profiles would be difficult to realize in practice, they have the mathematical advantage of furnishing explicit expressions with which the predictions of the asymptotic analysis can be compared.

A piecewise-constant density profile of type (2) or (2′) is

$$\frac{\rho_1(z)}{\rho_0} = \begin{cases} 0, & |z| > l, \\ A, & |z| < l, \end{cases}$$

with $M_1 = -2Al$. The corresponding gradient is given by

$$\frac{1}{\rho_0}\frac{\mathrm{d}\rho_1}{\mathrm{d}z} = \frac{M_1}{2l}[\delta(z-l)-\delta(z+l)]. \tag{6.22}$$

Substitution into (6.1), use of the special properties of $\delta(z)$ and subsequent inversion gives

$$W(z) = \frac{g\alpha^2 M_1}{2\nu D l}[W(l)f_0(z-l)-W(-l)f_0(z+l)],$$

where we have used the identity $\mathscr{F}^{-1}[\hat{f}_0(\omega)\exp(\mathrm{i}\omega c)] = f_0(z-c)$ with $c = \pm l$. Validity of this expression for $W(z)$ at $z = \pm l$ leads to two homogeneous linear equations in $W(l)$ and $W(-l)$ which determine M_1 as an eigenvalue, thereby yielding the exact formula

$$\frac{g\alpha^2|M_1|}{\nu D} = 2l\{[f_0(0)]^2-[f_0(2l)]^2\}^{-\frac{1}{2}}. \tag{6.23}$$

It is worth noting that the formalism embodied in the functions $f_k(z)$ represents a very efficient way of arriving at (6.23). The standard approach to this type of problem, as exemplified by previous analyses of Rayleigh–Taylor instability, would involve expressions for W as linear combinations of the six linearly independent solutions of equation (2.11) with zero right-hand side, valid in each z-interval where $\mathrm{d}\rho_1/\mathrm{d}z \equiv 0$. A disturbance mode that decays to zero as $|z| \to \infty$ would then involve three unknown coefficients for each semi-infinite body of fluid, and six for the central layer. Determination of M_1 would require evaluation of a 12×12 determinant derived from matching conditions imposed at the interfaces at $z = \pm l$. Our approach, a by-product of the asymptotic analysis, reduces this to a much more manageable 2×2 determinant.

For the representation

$$\frac{\rho_1(z)}{\rho_0} = \begin{cases} 0, & |z| > l, \\ -A, & 0 < z < l, \\ A, & -l < z < 0 \end{cases}$$

of case (3) ($A > 0$) and (3′) ($A < 0$), M_2 is equal to $2Al^2$, and the density gradient assumes the form

$$\frac{1}{\rho_0}\frac{\mathrm{d}\rho_1}{\mathrm{d}z} = \frac{M_2}{2l^2}[\delta(z+l) - 2\delta(z) + \delta(z-l)]. \tag{6.24}$$

Manipulations of the same type as before lead to the equations

$$\left.\begin{aligned} \{[f_0(l)]^2 - \tfrac{1}{2}f_0(0)[f_0(0)+f_0(2l)]\}\left(\frac{g\alpha^2 M_2}{\nu D l^2}\right)^2 + \tfrac{1}{2}[f_0(0) - f_0(2l)]\left(\frac{g\alpha^2 M_2}{\nu D l^2}\right) + 1 = 0, \\ \frac{g\alpha^2 M_2}{\nu D l^2} = \frac{2}{f_0(0) - f_0(2l)}. \end{aligned}\right\} \tag{6.25}$$

The two roots of the quadratic equation correspond to the even modes for cases (3) and (3′), and the second equation applies to the odd mode for case (3).

Equations (6.23) and (6.25) represent exact relations applicable to arbitrary values of the parameters. Numerical and algebraic calculations for these examples where ρ_1 is piecewise constant confirm that the asymptotic analysis correctly predicts the limiting dependence of the Rayleigh number upon αl for neutral stability and $\alpha l \ll 1$ (cf. equations (6.12), (6.15), (6.17) and (6.21)), as well as the limiting functional dependence of γ upon α at small Rayleigh numbers (cf. equations (6.11) and (6.14)). This serves as a check on the approximate approach.

6.3. *Numerical solution of equation* (2.11) *for representative density profiles of types* (1)–(3)

As representative density profiles for more detailed numerical study we have selected the following forms related to the Gaussian function for cases (1), (2) and (3) respectively:

$$\frac{\rho_1(z)}{\rho_0} = AF(z/l), \quad AF'(z/l), \quad AF''(z/l), \tag{6.26}$$

where

$$F(\zeta) = \tfrac{1}{2}\operatorname{erf}\zeta = \pi^{-\frac{1}{2}}\int_0^{\zeta} \mathrm{e}^{-s^2}\,\mathrm{d}s \tag{6.27}$$

and a prime denotes differentiation with respect to the argument $\zeta = z/l$. These are the functional forms drawn in figure 7.

A numerical approach necessarily involves some element of truncation, and we have elected to introduce stress-free constant-density boundaries at planes $z = \pm\mathscr{L}$ far removed from the central layer (cf. Matthews 1988). For sufficiently large $\mathscr{L}$, the Rayleigh number R^{b} and growth exponent γ^{b} calculated for the bounded system (distinguished by superscript b) are expected to be good approximations to the corresponding stability properties for the original unbounded system, as demonstrated by Matthews for his cellular flow patterns. The convergence as $\mathscr{L} \to \infty$ will be slower here, however, because fluid of constant density above and below is less effective at suppressing the disturbance than stably stratified fluid and the flow decays exponentially on the lengthscale α^{-1} (cf. figure 8). Thus, $\mathscr{L}$ needs to be large compared with the horizontal wavelength in order not to affect global disturbances.

For given $\mathscr{L}$, an even disturbance mode $W(z)$ is expanded in the series (4.2). Substitution into (2.11), multiplication through by any one term of the series and subsequent integration from 0 to $\mathscr{L}$ with respect to z leads ultimately to an infinite homogeneous system of linear equations of the form

$$[\lambda \boldsymbol{I} - (\alpha l)^{-4}\boldsymbol{B}]\,\boldsymbol{W} = 0, \tag{6.28}$$

where $\lambda = \nu D/gAl^3$ is the eigenvalue, $\boldsymbol{W} = (W_1, W_2, \ldots)$ is the corresponding vector of expansion coefficients, $\boldsymbol{I}$ is the identity matrix and the matrix $\boldsymbol{B}$ is given by

$$B_{mn} = (2P_m)^{-1}(f_{m+n-1} + f_{m-n}), \tag{6.29}$$

with

$$P_m = \left\{\frac{\gamma}{D\alpha^2} + 1 + \frac{\pi^2(m-\frac{1}{2})^2}{(\alpha\mathscr{L})^2}\right\}\left\{\frac{\gamma}{\nu\alpha^2} + 1 + \frac{\pi^2(m-\frac{1}{2})^2}{(\alpha\mathscr{L})^2}\right\}\left\{1 + \frac{\pi^2(m-\frac{1}{2})^2}{(\alpha\mathscr{L})^2}\right\} \tag{6.30}$$

and

$$f_k = \frac{2l}{A\mathscr{L}}\int_0^{\mathscr{L}} \frac{1}{\rho_0}\frac{\mathrm{d}\rho_1}{\mathrm{d}z}\cos\left(\frac{k\pi z}{\mathscr{L}}\right)\mathrm{d}z. \tag{6.31}$$

Substitution of the expressions (6.26) into (6.3) shows that the relation between the eigenvalue λ and the Rayleigh numbers defined in (6.9), (6.15) and (6.17) is $R = \lambda^{-1}$ in case (1), $R = 2\lambda^{-1}$ in case (3), and $R = -2\lambda^{-1}$ in case (3′). For global modes these relations involve the largest positive eigenvalue in cases (1) and (3) or the negative eigenvalue of largest magnitude in case (3′). Accurate approximate expressions for the coefficients (6.31) can be derived using contour integration techniques. Matthews (1988) determined the Rayleigh number for neutral stability as the smallest (real, positive) zero of the determinant corresponding to a truncation of a system equivalent to (6.28). For large matrices, calculation of the determinant (here using a linear equation solver) represents a viable approach, as we have checked, but probably not the most efficient. We have therefore generally opted to compute values of the Rayleigh number from the appropriate eigenvalue of $\boldsymbol{B}$, the latter being determined with the help of EISPACK subroutines (Dongarra & Moler 1984).

The generation of accurate numerical results requires consideration of two criteria. First, one must choose $\mathscr{L}$ so large that the pertinent eigenvalue of the bounded system is close to the actual eigenvalue of the unbounded system. The preceding asymptotic analysis indicates that, for neutral disturbances at small αl, W invariably decays as $(\alpha z)^N \exp(-\alpha z)$ where $N = 1$ or 2. Thus, smallness of $(\alpha\mathscr{L})^N \exp(-\alpha\mathscr{L})$ ensures that W has decayed more-or-less completely when the free surface is reached; our numerical calculations were performed with $\alpha\mathscr{L} = 10$. Second, for given $\mathscr{L}$ one should operate with sufficiently many modes. The first zero of the Mth mode occurs at $z \approx \mathscr{L}/2M$. Resolution of structure on the scale l would require this quantity to be small compared with l. The calculations indicate that $M \approx \mathscr{L}/l$ is already sufficiently large for purposes of calculating the first one or two eigenvalues (in which we are primarily interested), corresponding to the least oscillatory even eigenfunctions. It is evident that the numerical approach involves large matrices for small values of αl, and therefore demands more computational power as $\alpha l \to 0$. Fortunately, this is precisely the regime where the asymptotic analysis becomes accurate. In conjunction, the asymptotic and numerical approaches allow quantitative analysis of disturbances at arbitrary wavelengths.

The preceding discussion has been restricted to disturbance flows symmetric about the central layer (i.e. even functions of z). We have also encountered odd modes (case 3) and asymmetric modes (cases 2, 2′). The same type of numerical technique applies provided one utilizes a sine series and, most generally, the series

$$W = \sum_{k=1}^{\infty} W_k^{(c)} \cos[\pi(k-\tfrac{1}{2})z/\mathscr{L}] + \sum_{k=1}^{\infty} W_k^{(s)} \sin(\pi k z/\mathscr{L}). \tag{6.32}$$

Separate schemes were devised for these other cases, but the preceding paragraphs indicate the nature of the calculations and it is not necessary to present the details.

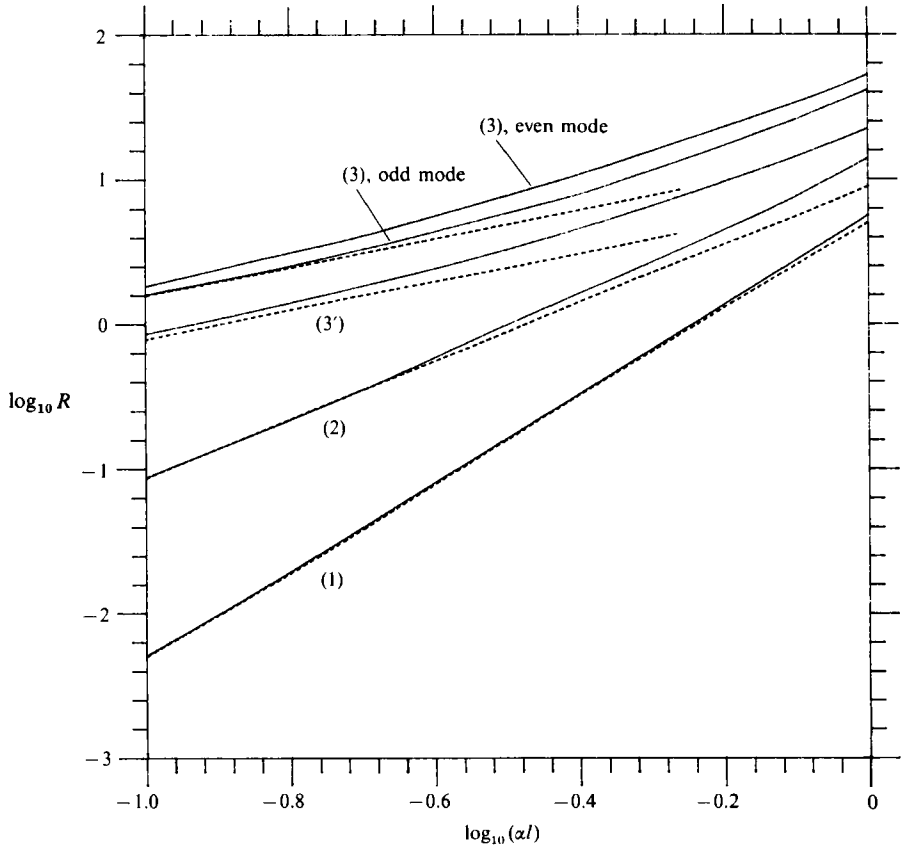

FIGURE 11. Dependence of the Rayleigh number for neutral stability on the horizontal wavenumber α for density variations of types (1), (2), (3), (3′). The continuous lines represent values calculated for the representative functional forms (6.26) by numerical solution of equation (2.11). Broken lines represent the limiting power laws predicted by the asymptotic analysis for $\alpha l \to 0$.

Figure 11 compares computed values of the Rayleigh number for neutral stability with the predictions of equations (6.9), (6.12), (6.15) and (6.17), and shows clearly the approach of the 'exact' values to the corresponding leading asymptotic behaviour. Figure 12(*a–d*) illustrates, for all the cases considered, the computed dependence of the growth rate γ on the horizontal wavenumber α for fixed values of the pertinent Rayleigh number. Although these graphs have the same general appearance as those in figures 9 and 10, their significance is different. The curves in figures 9 and 10 refer to circumstances in which the central layer is negligibly thin and its thickness does not enter explicitly into the computed Rayleigh number or growth rate. Thus, figures 9 and 10 represent, in different dimensionless variables, an expanded view of figure 12(*a–d*) in the vicinity of the origin, corresponding to small values of the Rayleigh number. Figure 12(*a–d*) is not restricted to the universal asymptotic properties of the various types of density distribution at small Rayleigh numbers. Rather, it shows for the simple representative density profiles (6.26) the effect of finite layer thickness (αl not very small). It is seen that appreciable thickness of the central layer reduces the growth rate and increases the Rayleigh number for neutral stability relative to the leading-order asymptotic values, and therefore represents a stabilizing factor. This conclusion agrees with the qualitative predictions of the higher-order asymptotic

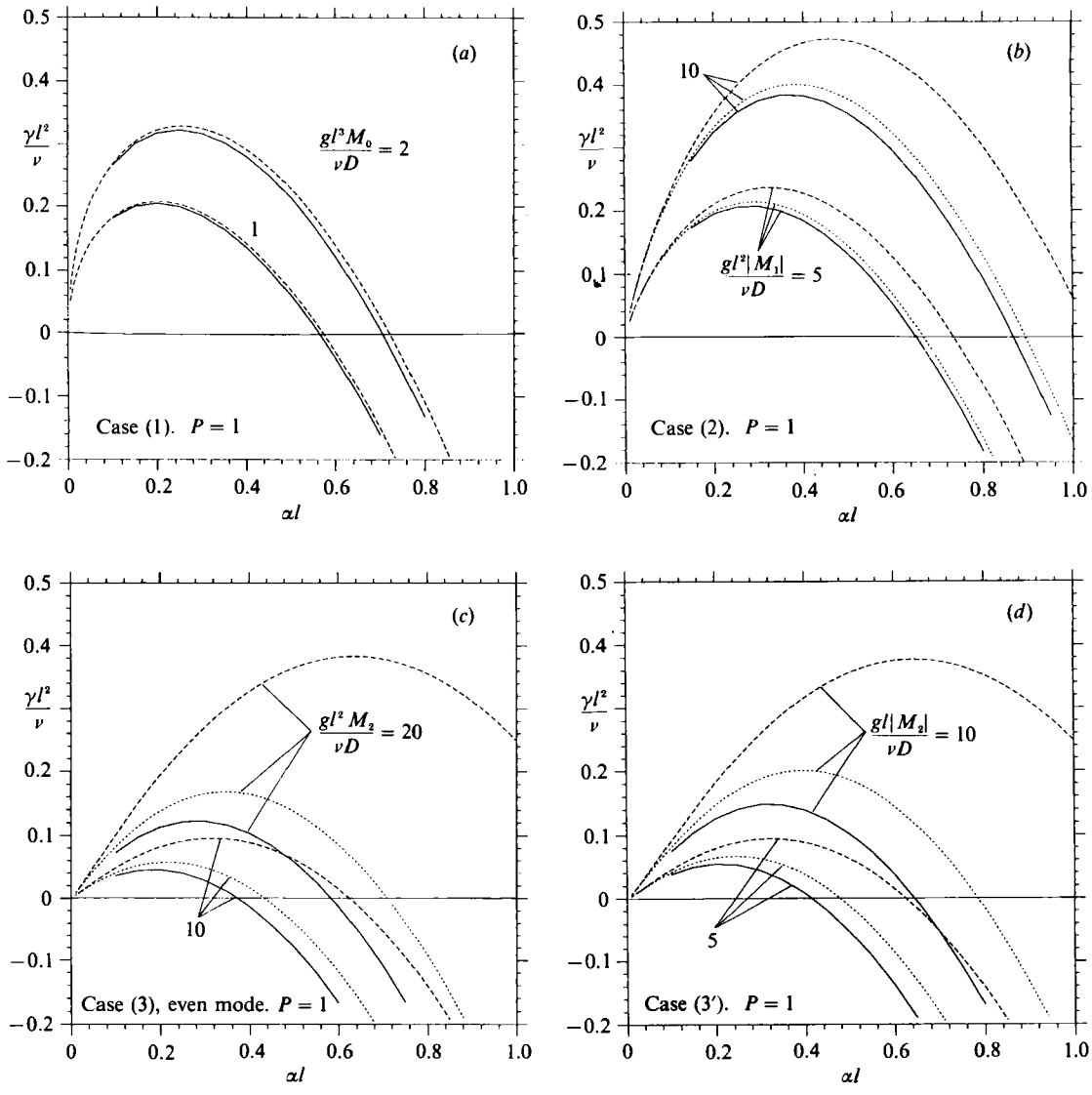

FIGURE 12. Growth rate γ as a function of the horizontal wavenumber α for density stratification of types (1), (2), (3) and (3′). Continuous curves represent numerical values for the functional forms (6.26). Broken curves in (*a*), (*b*), (*c*) and (*d*) represent the relations (6.8), (6.11), (6.14) and (6.14) respectively derived from the leading-order asymptotic analysis valid when $\alpha l \ll 1$. The additional dotted curves for case (2) correspond to the piecewise-constant density profile (6.22), and those for cases (3) and (3′) correspond to (6.24). In every case $P = 1$. The curves for case (3), odd mode, are quantitatively similar to those for the even mode.

analysis. Comparison of the curves corresponding to the piecewise-constant (dotted curves) and Gaussian-derived (continuous curves) density variations shows that discontinuities have a destabilizing influence, although appreciable thickness of the central layer decreases the growth rate for these two kinds of profile relative to the curves given by the asymptotic analysis.

7. The energy balance for a disturbance with large horizontal wavelength when $\nu = 0$ and $D = 0$

For mathematical reasons the analysis in §6 was limited to small values of the Reynolds number $\gamma l^2/\nu$, a limitation which is not serious in an examination of neutral and adjoining disturbances. We consider now the other extreme case in which the Reynolds number $\gamma l^2/\nu$ is large, so that the motion is effectively inviscid and also diffusionless† (assuming D/ν is not too large) everywhere. It is possible to give a simple physical description of the disturbance motion under these conditions from which values of the growth rate γ may easily be derived by considering the balance of kinetic and gravitational potential energy. This physical picture is applicable to all those undisturbed states that we have found to be markedly unstable to global disturbances which tilt the layers of non-uniform density and cause sliding of the fluid within the layers, viz. the case of a sinusoidal density distribution (§5) and cases in which ρ_1 differs from zero only in a central layer (§6).

We note first that when $\nu = 0$ and $D = 0$ the governing equation (2.11) reduces to the second-order equation

$$\frac{\mathrm{d}^2 W}{\mathrm{d}z^2} + \alpha^2 W\left(\frac{g}{\gamma^2 \rho_0}\frac{\mathrm{d}\rho_1}{\mathrm{d}z} - 1\right) = 0, \tag{7.1}$$

where, as before, the vertical component of velocity of a normal mode has been written as

$$w = W(z)\,\mathrm{e}^{\gamma t}\cos\alpha x \tag{7.2}$$

and α is the horizontal wavenumber of the disturbance. The wavelength $2\pi/\alpha$ will be assumed to be large compared with any length characteristic of the undisturbed density distribution, and it follows from (7.1) that W is a slowly varying function of z on the scale of that length.

7.1. *The case* $\rho_1 = \rho_0 A \sin\kappa z$

We take it for granted that here the most unstable disturbance is such that W is periodic with respect to z, with period $2\pi/\kappa$, and is an even function of z. There is no actual need in this case for a new method of analysis because the formulae (5.17) and (5.18) are valid for any Rayleigh number and give the growth rate as

$$\gamma = 2^{-\frac{1}{4}}(\alpha g A)^{\frac{1}{2}} \tag{7.3}$$

when $\nu = D = 0$ and $\alpha/\kappa \ll 1$. The relation between γ and α here is the same as for Rayleigh–Taylor instability. Moreover there exists an explicit solution of (7.1), now the Mathieu equation, which is periodic with period $2\pi/\kappa$ and for which (7.3) may readily be seen to be the characteristic-value equation when $\alpha/\kappa \ll 1$ (Whittaker & Watson 1915, §19.3). However, we shall apply the energy-balance method to the case of a sinusoidal density distribution in order to gain more insight into the global instability mechanism, and relations like (7.3) will serve as a check on its correctness.

Consider first the total kinetic energy of the disturbed fluid at time t. The vertical component of velocity of the fluid is given by (7.2), in which $W(z)$ is approximately constant, and equal to W_0 say, when $\alpha/\kappa \ll 1$. To obtain the horizontal component u we construct the equation of motion of a thin material sheet of fluid which in the

† Note that there is no problem about the assumption of a steady undisturbed state in this case.

undisturbed state is planar and horizontal at vertical position z. In the disturbed state the vertical displacement of the sheet at horizontal position x is

$$\eta = \frac{W_0}{\gamma} e^{\gamma t} \cos \alpha x, \tag{7.4}$$

in conformity with (7.2). The sheet is now locally inclined to the horizontal at a small angle $\partial\eta/\partial x$, and the fluid of excess density ρ_1 in the sheet slides freely, either down if $\rho_1 > 0$ or up if $\rho_1 < 0$, with a local velocity q given (after use of the Boussinesq approximation) by

$$\rho_0 \frac{\partial q}{\partial t} = -g\rho_1 \frac{\partial \eta}{\partial x},$$

whence

$$u = \frac{\alpha g A}{\gamma^2} W_0 e^{\gamma t} \sin \alpha x \sin \kappa z \tag{7.5}$$

correct to the first order in disturbance quantities. The kinetic energy of the fluid per wavelength $2\pi/\alpha$ in the x-direction, per wavelength $2\pi/\kappa$ in the z-direction, and per unit depth in the y-direction, is thus

$$\begin{aligned} T &= \frac{\alpha\kappa}{4\pi^2} \int_0^{2\pi/\alpha} \int_0^{2\pi/\kappa} \tfrac{1}{2}\rho_0 (1 + A \sin \kappa z)(u^2 + w^2)\, dx\, dz \\ &= \tfrac{1}{4}\rho_0 W_0^2 e^{2\gamma t} \left(\frac{\alpha^2 g^2 A^2}{2\gamma^4} + 1 \right). \end{aligned} \tag{7.6}$$

The other form of energy is gravitational potential energy, which for the same body of fluid is increasing at the rate

$$\frac{dP}{dt} = \frac{\alpha\kappa}{4\pi^2} \int_0^{2\pi/\alpha} \int_0^{2\pi/\kappa} w(\rho_1 + \rho')\, g\, dx\, dz. \tag{7.7}$$

In the absence of diffusion (2.8) reduces to

$$\rho' = -\frac{w}{\gamma} \frac{d\rho_1}{dz}, \tag{7.8}$$

which may be substituted in (7.7). Only the density fluctuation contributes to the integral with respect to x in (7.7), and we obtain

$$\frac{dP}{dt} = -\frac{\kappa^2 \rho_0 g A}{4\pi\gamma} e^{2\gamma t} \int_0^{2\pi/\kappa} W^2 \cos \kappa z\, dz. \tag{7.9}$$

Our approximation that $W(z)$ is constant is too crude here, because it omits the small but vital vertical component of velocity due to the sliding of the fluid sheets. A better approximation, obtained from (7.5) and the mass-conservation relation $\partial w/\partial z = -\partial u/\partial x$, is

$$W(z) = W_0 \left(1 + \frac{\alpha^2 g A}{\kappa \gamma^2} \cos \kappa z \right).$$

When this is substituted in (7.9) we get

$$\frac{dP}{dt} = -\frac{\alpha^2 g^2 A^2}{2\gamma^3} \rho_0 W_0^2 e^{2\gamma t}.$$

The energy balance requires that $\mathrm{d}(T+P)/\mathrm{d}t = 0$, where T is given by (7.6), whence we recover the known expression (7.3) for the growth rate γ. It is noteworthy that this expression is independent of κ. This results from the fact that every initially horizontal fluid sheet is deformed and develops a sliding motion in the same way regardless of the vertical distribution of density.

7.2. *The case in which $\rho_1 = 0$ except in a central layer*

Again we calculate the total kinetic energy and rate of change of potential energy for a disturbance whose horizontal wavelength is large compared with the layer thickness. In this case the vertical velocity component is approximately uniform within the central layer, and we put $W(z) = W_1$ there. Outside the layer the motion is irrotational and the velocity potentials in the regions above and below the layer are

$$\phi = \mp \frac{W_1}{\alpha} \exp(\gamma t \mp \alpha z) \cos \alpha x.$$

The total kinetic energy of the fluid per unit wavelength in the x-direction and per unit length in the y-direction is thus approximately

$$T = \frac{1}{2\alpha} \rho_0 W_1^2 \mathrm{e}^{2\gamma t}, \tag{7.10}$$

the contribution from the relatively thin central layer being negligible.

The change in the potential energy on the other hand is dominated by the contribution from the central layer. Beginning again with (7.7) (but with the integration with respect to z now over all values of z) and using (7.8) we find

$$\begin{aligned} \frac{\mathrm{d}P}{\mathrm{d}t} &= -\frac{\alpha g}{2\pi\gamma} \int_0^{2\pi/\alpha} \int_{-\infty}^{\infty} w^2 \frac{\mathrm{d}\rho_1}{\mathrm{d}z} \mathrm{d}x \, \mathrm{d}z \\ &= -\frac{\alpha g}{\pi\gamma} \int_0^{2\pi/\alpha} \int_{-\infty}^{\infty} w \frac{\partial u}{\partial x} \rho_1 \mathrm{d}x \, \mathrm{d}z. \end{aligned} \tag{7.11}$$

The sliding velocity of a fluid sheet in the central layer, analogous to (7.5), is

$$u = \frac{\alpha g \rho_1}{\gamma^2 \rho_0} W_1 \mathrm{e}^{\gamma t} \sin \alpha x, \tag{7.12}$$

and when the expressions (7.2) and (7.12) are substituted for w and u (7.11) becomes

$$\frac{\mathrm{d}P}{\mathrm{d}t} = -\frac{\alpha^2 g^2}{\gamma^3} \rho_0 W_1^2 \mathrm{e}^{2\gamma t} \int_{-\infty}^{\infty} \frac{\rho_1^2}{\rho_0^2} \mathrm{d}z. \tag{7.13}$$

The requirement of zero rate of change of the total energy $T+P$ then gives the approximate result

$$\gamma^4 = \alpha^3 g^2 \int_{-\infty}^{\infty} \frac{\rho_1^2}{\rho_0^2} \mathrm{d}z, \tag{7.14}$$

valid when $\alpha l \ll 1$ and $\gamma l^2/\nu \gg 1$. The parameter of the undisturbed density distribution that determines the growth rate is different from that at the small Reynolds numbers investigated in §6. In particular there is here no qualitative difference between zero and non-zero values of the total excess mass in the central layer. For the illustrative case

$$\frac{\rho_1}{\rho_0} = \frac{A}{\pi^{\frac{1}{2}}} \exp\left(-\frac{z^2}{l^2}\right)$$

the growth rate is $$\gamma^4 = (2\pi)^{-\frac{1}{2}}\alpha^3 lg^2 A^2. \tag{7.15}$$

The isolated central layer of non-uniform density is slightly less unstable than a sinusoidal density distribution inasmuch as the growth rate in the former case is smaller, by a factor of order $(\alpha l)^{\frac{1}{4}}$, than that in the latter case.

With regard to the requirement of high Reynolds number of the disturbance flow, we see from (7.15) that this amounts to

$$\frac{\gamma l^2}{\nu} \sim (\alpha l)^{\frac{3}{4}} R^{\frac{1}{2}} \gg 1,$$

where $R = gAl^3/\nu^2$ is the Rayleigh number (for Prandtl number unity) based on the layer thickness. The physical conditions required for satisfaction of this inequality are not extreme; it would be satisfied, for example, in the case of a layer of thickness 1 cm in water with a density variation given by $A = 0.01$ and a wavenumber $\alpha l = 0.1$. The value of the analysis for an inviscid fluid without diffusion lies also in its simple demonstration of the mechanism of the instability.

We are grateful to Professor S. H. Davis of Northwestern University and Professor C.-S. Yih of the University of Michigan for drawing our attention to the possible relevance of Floquet theory. Support from the US National Science Foundation in the form of an NSF-NATO Post-doctoral Fellowship to J.M.N. is gratefully acknowledged.

REFERENCES

BATCHELOR, G. K. 1988 A new theory of the instability of a uniform fluidized bed. *J. Fluid Mech.* **193**, 75–110.

BATCHELOR, G. K. 1991 The formation of bubbles in fluidized beds. *Proc. of Symposium honoring John W. Miles on his 70th birthday.* Scripps Institution of Oceanography, Reference Series 91.

BELLMAN, R. & PENNINGTON, R. H. 1954 Effects of surface tension and viscosity on Taylor instability. *Q. Appl. Maths* **12**, 151–162.

CHANDRASEKHAR, S. 1961 *Hydrodynamic and Hydromagnetic Stability.* Oxford University Press.

DONGARRA, J. J. & MOLER, C. B. 1984 EISPACK – a package for solving matrix eigenvalue problems. *Argonne National Laboratory, Math. & Comp. Sci. Div., Tech. Memo.*

GRIBOV, V. N. & GUREVICH, L. E. 1957 On the theory of the stability of a layer located at a superadiabatic temperature gradient in a gravitational field. *Sov. Phys. JETP* **4**, 720–729.

INCE, E. L. 1944 *Ordinary Differential Equations.* Dover.

JACKSON, R. 1963 The mechanics of fluidized beds. I The stability of the state of uniform fluidization. *Trans. Inst. Chem. Engrs* **41**, 13–21.

KYNCH, G. J. 1952 A theory of sedimentation. *Trans. Faraday Soc.* **48**, 166–176.

MATTHEWS, P. C. 1988 A model for the onset of penetrative convection. *J. Fluid Mech.* **188**, 571–583.

TAYLOR, G. I. 1950 The instability of liquid surfaces when accelerated in a direction perpendicular to their planes. I. *Proc. R. Soc. Lond.* A **201**, 192–196.

WHITTAKER, E. T. & WATSON, G. N. 1915 *A Course of Modern Analysis.* Cambridge University Press.

YIH, C.-S. 1959 Thermal instability of viscous fluids. *Q. Appl. Maths* **17**, 25–42.